High Dimensionality Reduction by Matrix Factorization for Systems Pharmacology

Adel Mehrpooya[1,4], Farid Saberi-Movahed[*,2], Najmeh Azizizadeh[3], Mohammad Rezaei-Ravari[4], Mahdi Eftekhari[*,4], and Iman Tavassoly[*,5,†]

[1]School of Mathematical Sciences, Science and Engineering Faculty, Queensland University of Technology (QUT), Brisbane, Australia
[2]Department of Applied Mathematics, Faculty of Sciences and Modern Technologies, Graduate University of Advanced Technology, Kerman, Iran
[3]Department of Applied Mathematics, Faculty of Mathematics and Computer, Shahid Bahonar University of Kerman, Iran
[4]Department of Computer Engineering, Faculty of Engineering, Shahid Bahonar University of Kerman, Kerman, Iran
[5]Department of Pharmacological Sciences, Icahn School of Medicine at Mount Sinai, New York, USA

Abstract

The extraction of predictive features from the complex high-dimensional multi-omic data is necessary for decoding and overcoming the therapeutic responses in systems pharmacology. Developing computational methods to reduce high-dimensional space of features in *in vitro*, *in vivo* and clinical data is essential to discover the evolution and mechanisms of the drug responses and drug resistance. In this paper, we have utilized the Matrix Factorization (MF) as a modality for high dimensionality reduction in systems pharmacology. In this respect, we have proposed three novel feature selection methods using the mathematical conception of a basis. We have applied these techniques as well as three other matrix factorization methods to analyze eight different gene expression datasets to investigate and compare their performance for feature selection. Our results show that these methods are capable of reducing the feature spaces and find predictive features in terms of phenotype determination. The three proposed techniques outperform the other methods used and can extract a 2-gene signature predictive of a Tyrosine Kinase Inhibitor (TKI) treatment response in the Cancer Cell Line Encyclopedia (CCLE).

Keywords: Cancer, Cancer Cell Line Encyclopedia, Dimension Reduction, Feature Selection, Matrix Factorization, Systems Pharmacology

[*]Corresponding authors: tavassoly@gmail.com, m.eftekhari@uk.ac.ir and f.saberimovahed@kgut.ac.ir
[†]Iman Tavassoly contributed to this paper at the Cellular Energetics Program of the Kavli Institute for Theoretical Physics (KITP), Santa Barbara, USA.

1 Introduction

One of the challenges in the era of systems medicine is to decode and select personalized features for an individual patient to design personalized therapeutic regimens [1, 2], even if the disease has been modeled analytically [3, 4, 5, 6]. Although systems pharmacology-based mechanistic models which are built based on the known interactions among molecular mechanisms and phenotypes provide a path to solve this problem, but high dimensionality of clinical and molecular characteristics, including multi-omic features, adds more complexity to uncovering the mechanisms causing complex diseases in any model system and patient [7]. Systems-level study of interaction networks constructed from omics data can lead to static models connecting molecular data to phenotypes [8]. Yet, these types of models are still high-dimensional and lack temporal characteristics of disease evolution. A path to design personalized molecular sets assigned to a specific phenotype of a complex disease like cancer is to use phenomenological approaches to reduce the high-dimensional data [9]. The emergence of molecular signatures on this domain requires new methodologies for both model reduction and feature selection in large molecular omic and multi-omic data sets. In systems pharmacology, predicting the therapeutic responses in *in vitro* and *in vivo* models and detecting the molecular signatures related to drug resistance help to narrow down the therapeutic regimens for testing in clinical trials [1, 10]. High-dimensional data has noise and redundancy and includes irrelevant information controlled by some unknown parameters required for the model to run. For this reason, analysis of large biological data sets does not always end in robust models and is computationally costly while being prone to over-fitting [11, 12]. In addition, if the modeling process is selected to stand on the distance between molecular features, the designed methods face even more performance degeneration due to adverse impacts of the high-dimensional feature space on the calculation of feature distances. With the emergence of advanced information technology and its increasing applications in electronic communications, a wide variety of modern devices have been designed based on big data whose dimension is exceptionally high [13, 14, 15]. The noise and redundancy, including the irrelevant information, come from a large number of complex parameters in the model, and it results in a limited ability to generalize the learning model and impose inefficient requirements such as more memory usage and longer processing time on the computational devices since the corresponding algorithms suffer enormously from over-fitting [16, 17, 18, 19, 20, 21].

To face the challenge of high dimensionality, two well-known approaches have been proposed. One of these methods is ”Feature Extraction” which reduces the dimension by projecting the data given in a higher-dimensional space, through a proper mapping, into a subspace of this space whose dimension is lower enough than that of the original space [22, 23, 24, 25, 26]. The other technique is ”Feature Selection” which reduces the high dimensionality by selecting a smaller number of features compared to the original feature set so that the selected features have the capability to represent the original feature space optimally [27, 28, 29]. It is proved that both techniques, particularly feature selection, substantially contribute to eliminate redundancy and noise, remove the irrelevant parameters and enhance the efficiency of data analysis computations, thus leading to a decrease in the costs associated with time and storage [30, 31]. This way, feature extraction, and feature selection provide considerable improvements in the clustering and classification accuracy, respectively. It should be pointed out that feature selection maintains the original features' conceptual information by preserving the original features representation more perfectly compared to feature extraction, which constructs new features. For this reason, it is more common to use feature selection than feature extraction to develop novel algorithms for handling dimension reduction tasks in recent years [22, 32].

A broad and significant category of the applications of machine learning techniques discussed can be merged with systems pharmacology methodologies to uncover the quantitative features involved in the evolution and treatment of complex diseases such as cancers [1]. One of the first steps to build systems pharmacology models and platforms is to analyze big datasets such as gene expressions and transcriptomics. Since these datasets, considering phenotypes associated with them, are big and complex datasets, reducing their high dimensionality is a key to be able to use them in systems pharmacology [1]. For instance, to determine the sensitivity and resistance to a specific therapeutic *in vitro* and *in vivo*, it is necessary to explore the bio-molecular datasets such as gene expression profiles of hundreds of cancer cell lines [2]. Exploring these datasets to extract features related to the mechanisms causing therapeutic-resistant phenotype requires reducing the high-dimensional space of the molecular features. The complexity of the omic datasets, including gene expressions, originates from two major properties of the biological systems. The first one is intrinsic geometry. It indicates the geometrical properties of these data need to be preserved when the features initially exist in a manifold of high-dimension mapped into a lower-dimension sub-manifold of the base space. The other characteristic of such big data is the noise and enormous amount of outliers.

Over the past decades, subspace learning techniques have demonstrated a considerable ability to deal with feature selection problems and their applications to the analysis of complex biological systems [12, 33, 34, 35, 36]. It is required that the subspace learning techniques and feature selection methods, particularly when they are employed to handle gene expression data, are equipped with some proper and efficient tools. In this regard, some modifications have been incorporated into these methods. One notable example is subspace learning for unsupervised feature selection via matrix factorization (MFFS), introduced in [37], in which a subspace learning framework is designed from the perspective of the matrix decomposition. Thereupon, the MFFS framework and the idea of minimum redundancy were merged to adapt unsupervised feature selection via maximum projection and minimum redundancy (MPMR) [38]. Another interesting example is subspace learning-based graph regularized feature selection (SGFS), investigated in [39], which can maintain the features intrinsic information in terms of features geometry. Then utilizing matrix factorization techniques again, an unsupervised method, feature selection based on maximum projection and minimum redundancy (MPMR), was explored. It is apparent that the aforementioned algorithms are able to provide a highly accurate estimate of the feature space by learning a proper subspace and can also produce satisfactory outcomes for the corresponding feature selection task.

Although the mentioned methods provide powerful tools to successfully develop new practical models for dimension reduction problems, they have not been vastly applied to systems pharmacology. The major goal of this paper is to establish a number of novel feature selection frameworks and apply them to cancer gene expression data. In the proposed methods, not only are the notable and outstanding achievements of the MFFS, MPMR and SGFS methods considered, but also the performance of the introduced methods is improved in terms of classification and clustering tasks. To this aim, the notion of a basis, which is an essential concept in the theory of linear vector spaces, is applied. Normally, a basis possesses two fundamental characteristics, each of which has a positive and constructive impact on the discriminative feature selection process [35]. The first property is that a basis generates the whole feature space making use of the basis elements. This means that the characteristics of original features are included in the basis whose number of elements is far smaller than that of the whole feature space. A major achievement of this issue is that rather than considering the original features, a basis can be utilized to represent them which results in a noticeable reduction in the number of the selected features and the calculating processes. The second property of a basis is that its elements are linearly

independent, which indicates a significant decrease of the level of redundancy in data.

Figure 1 illustrates a schematic diagram of the major set of concepts employed in the proposed methods. It can be seen from this diagram that considering an original feature data, a basis of features is firstly built for the original feature space. Correspondingly, the feature selection problem is defined based on the constructed basis. Through some regularizers such as "the $L_{2,1}$-norm sparsity regularization", "the redundancy of the basis space" and "the manifold of the basis space", three feature selection methods are introduced under these regularizations, and the feature matrix $\mathbf{W}$ is learned to enhance the feature learning performance.

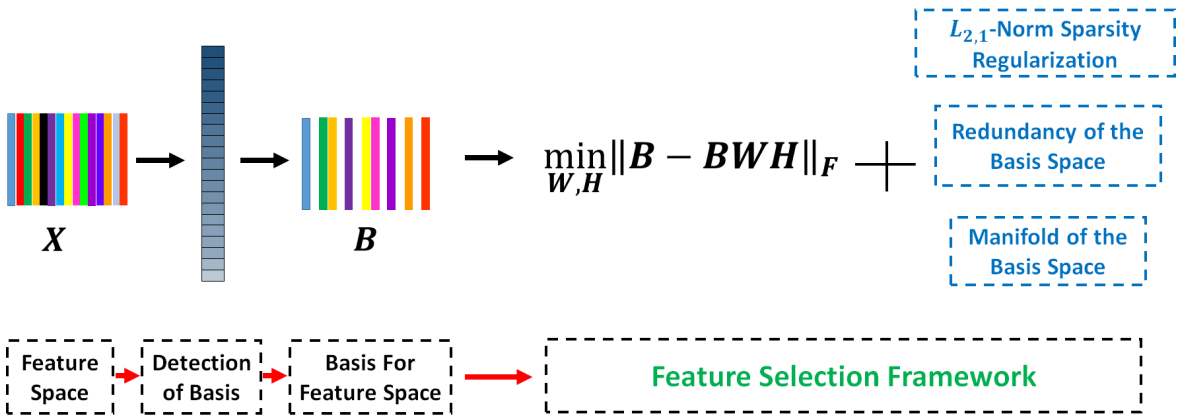

Figure 1: A schematic diagram of the fundamental framework of the proposed methods.

2 Methods

2.1 Preliminaries and Notations

Throughout the paper, lowercase letters in Italic are used to denote the scalers, uppercase letters in boldface represent matrices, lowercase letters in boldface indicate vectors, and uppercase letters in italic are used for sets. For a matrix $\mathbf{A}$, the set including all linear combinations of its columns is denoted by $\mathrm{span}(\mathbf{A})$. $\mathbf{E}_k$ represents the $k \times k$ identity matrix. For a square matrix $\mathbf{A}$, $\mathbf{A}^T$ and $\mathrm{Tr}(\mathbf{A})$ denote the transpose and the trace operators, respectively. In addition, $\|\mathbf{A}\|_F$ is the Frobenius norm of the matrix $\mathbf{A}$. For a matrix $\mathbf{B} \in \mathbb{R}^{m \times n}$, the $L_{2,1}$–norm is given by $\|\mathbf{A}\|_{2,1} = \sum_{j=1}^{n} \sqrt{\sum_{i=1}^{m} \mathbf{A}_{ij}^2}$.

Furthermore, the data matrix is represented by $\mathbf{X} = [\mathbf{x}_1; \mathbf{x}_2; \ldots; \mathbf{x}_n] = [\mathbf{f}_1, \mathbf{f}_2, \ldots, \mathbf{f}_d] \in \mathbb{R}^{n \times d}$, where n and d indicate the number of samples and that of features, respectively. It is supposed that $n \leq d$. For a feature subset X_I, the corresponding submatrix of $\mathbf{X}$ is simply represented by $\mathbf{X}_I$ that is a matrix of order $n \times k$ in which I and $|I|$ indicate the index set of the selected features and the number of indices of I, respectively. Given a vector space V of dimension n, a basis for V is a subset $B = \{\mathbf{v}_1, \mathbf{v}_2, \ldots, \mathbf{v}_n\}$ of n linearly independent elements of V such that V is spanned by the vectors of B. Given the set of features $\mathbf{X} = \{\mathbf{f}_1, \mathbf{f}_2, \ldots, \mathbf{f}_d\}$, it is supposed throughout this article that the set B is composed of n elements and is a basis of the vector space spanned by $\mathbf{X}$ as well as assuming that $\mathrm{rank}(\mathbf{X}) = n$.

2.2 Motivation

Over the past recent years, the notion of directional distance between two subspaces has received much attention in learning problems regarding subspaces so that several feature selection methods have been established based on this idea.

Definition 1 (Directional Distance [37])**.** Given two matrices $\mathbf{S}_1 \in \mathbb{R}^{m\times n}$ and $\mathbf{S}_2 \in \mathbb{R}^{m\times p}$, the distance from $\mathcal{S}_1 = \mathrm{span}(\mathbf{S}_1)$ to $\mathcal{S}_2 = \mathrm{span}(\mathbf{S}_2)$ is calculated by:

$$\overrightarrow{d}(\mathcal{S}_1, \mathcal{S}_2) = \min_{\mathbf{H}\in\mathbb{R}^{p\times n}} \|\mathbf{S}_1 - \mathbf{S}_2\mathbf{H}\|_F^2. \tag{1}$$

One most well-known and practical technique for feature selection is presented in Problem 1 that is rested on the directional distance defined above and has been the center of attention as the foundation of a number of powerful state-of-the-art algorithms in recent years [34, 35, 36, 37, 38, 39].

Problem 1. Let $\mathbf{X} \in \mathbb{R}^{n\times d}$ and $k \in \mathrm{Z}^+$. Considering $\mathcal{I}$ as a feature index set for which $|\mathcal{I}| = k$, a feature selection problem is formulated by Eq. (2).

$$\mathcal{I} = \underset{I}{\mathrm{argmin}}\ \overrightarrow{d}(\mathcal{X}, \mathcal{X}_I) \quad \text{subject to} \quad |I| = k, \tag{2}$$

where $\mathcal{X} = \mathrm{span}(\mathbf{X})$ and $\mathcal{X}_I = \mathrm{span}(\mathbf{X}_I)$.

Saberi-Movahed et al. [35] studied the importance of the representation of features provided by the notion of a basis of $\mathrm{span}(\mathbf{X})$ in terms of the improvements that this representation makes on the feature selection performance in Problem 1. Specifically, two highly significant properties were investigated as follows.

(1) Let B be a basis of $\mathrm{span}(\{\mathbf{f}_1, \mathbf{f}_2, \ldots, \mathbf{f}_d\})$ and $\mathcal{B} = \mathrm{span}(\mathbf{B})$. Then

$$\overrightarrow{d}(\mathcal{X}, \mathcal{B}) = 0, \tag{3}$$

(2) Let $X_I \subseteq X$ be a feature subset. Then

$$\overrightarrow{d}(\mathcal{B}, \mathcal{X}_I) \leq \overrightarrow{d}(\mathcal{X}, \mathcal{X}_I). \tag{4}$$

Item (1) states that for a basis B of a feature subspace $\mathcal{X}$, its span, $\mathcal{B}$, can be selected as a representation of $\mathcal{X}$ since $\mathcal{B}$ coincide $\mathcal{X}$. Furthermore, Item (2) indicates that the representation of $\mathcal{X}$ with $\mathcal{B}$, i.e., assuming that $\mathcal{X} = \mathcal{B}$, encourages us to replace $\overrightarrow{d}(\mathcal{X}, \mathcal{X}_I)$ in Problem 1 by $\overrightarrow{d}(\mathcal{B}, \mathcal{X}_I)$ and it guarantees that this replacement will not make the results of data fitting worse than that of the original problem [35].

Considering the merits of a basis in feature selection problems, Saberi-Movahed et al. [35] proposed a new objective function, given by Eq. (5), in which the original feature space was represented by a basis of this space. Problem 2 summarizes this method which improved the method presented by Problem 1.

Problem 2. Let X be the original set of features and B be a basis of the span of X. In addition, $\mathcal{B} = \mathrm{span}(\mathbf{B})$ and $\mathcal{X}_I = \mathrm{span}(\mathbf{X}_I)$. Assuming that $\mathcal{I}$ is a set composed of k indices of the features, an objective function can be formulated as:

$$\min_{|I|=k} \overrightarrow{d}(\mathcal{B}, \mathcal{X}_I) = \min_{\mathbf{H}\in\mathbb{R}^{k\times n}} \|\mathbf{B} - \mathbf{X}_I\mathbf{H}\|_F^2. \tag{5}$$

Recently, a supervised feature selection technique, SFS-BMF, rested on Problem 2, was presented in [35] so that a basis of features was applied to the selection process. The superiority of this method over a set of benchmark techniques was demonstrated by conducting diverse experiments on a number of gene expression datasets. Inspired by satisfactory outcomes that supervised feature selection founded on the notion of a basis achieved, we investigate the impacts of this idea on the outcomes of feature selection problems in the unsupervised mode.

2.3 Proposed Frameworks

This section presents a set of novel and effective feature selection techniques rested on Problem (2) and the notion of a basis. In Section 2.3.1, an original unsupervised feature selection method is offered based on a basis of the feature space. In addition, Section 2.3.2 proposes a new unsupervised feature selection technique in which the redundancy among the features is minimized. Finally, Section 2.3.3 introduces another method for feature selection that preserves features' intrinsic geometry.

2.3.1 The B-MFFS Method

Over the past decades, a set of methods have been founded on the concept of matrix factorization, including Singular Value Decomposition (SVD) [40], Non-negative Matrix Factorization (NMF) [41] and Principal Components Analysis (PCA) [42]. Since such techniques were originally developed to handle feature extraction tasks, they are not always perform well enough when applied to feature selection problems. In specific, interpretation of the features determined by the mentioned methods in a subspace of lower dimension is not acceptable. One technique to deal with this problem was "Matrix Factorization criterion of Feature selection Subspace learning" (MFFS), proposed by Wang et al. [37], in which matrix factorization was employed to carry out feature selection. This method was constructed using the problem presented in Eq. (6). This method determines the optimal subset of features subject to the constraints imposed on its optimization problem.

$$\underset{\mathbf{W},\mathbf{H}}{\operatorname{argmin}} \|\mathbf{X} - \mathbf{XWH}\|_F \quad \text{subject to } \mathbf{W} \geq 0, \mathbf{W}^T\mathbf{W} = \mathbf{E_k}. \tag{6}$$

In MFFS, matrix factorization is constrained by an orthogonality condition which is hardly fulfilled in practice.

The current section aims to present a novel method, B-MFFS, for feature selection problems that is rested on the mathematical notion of a basis. In particular, the B-MFFS problem is constructed based on the idea of selecting a basis for the feature space as a representation of this space. This means that first, a basis is determined for the space of the original features. Then, to design an efficient and effective mechanism for feature selection, the B-MFFS algorithm represents the original feature space by the span of this basis and minimizes the distance between this span and the set of the selected features. In addition, making use of the $L_{2,1}$–norm, the matrix of feature weights is regulated to guarantee the sparsity of feature selection [43].

Let $\mathbf{X} = \{\mathbf{f}_1, \mathbf{f}_2, \ldots, \mathbf{f}_d\}$ be the set of the original features and $\mathbf{B} = [\mathbf{f}_1^b, \mathbf{f}_2^b \ldots, \mathbf{f}_n^b] \in \mathbb{R}^{n\times n}$ be a basis of the span of $\mathbf{X}$. Since for a given subset $\mathbf{X}_I$ of $\mathbf{X}$, there is a unique representation of $\mathbf{X}_I$ in the form of a linear combination of elements of $\mathbf{B}$, a decomposition of $\mathbf{X}_I$ exists as follows: $\mathbf{X}_I = \mathbf{BG}$, where $\mathbf{G} \in \mathbb{R}^{n\times k}$. Considering the aforementioned reduced forms for $\mathbf{X}$ and $\mathbf{X}_I$, the feature selection

problem for B-MFFS is formulated by Eq. (7).

$$\underset{\mathbf{G}\in\mathbb{R}^{n\times k},\mathbf{H}\in\mathbb{R}^{k\times n}}{\operatorname{argmin}} \|\mathbf{B}-\mathbf{BGH}\|_F^2+\alpha\|\mathbf{G}\|_{2,1}, \tag{7}$$

where α is a regularization parameter, and the $L_{2,1}$–norm is imposed on the feature selection matrix to guarantee that this matrix is sparse. Moreover, the term $\|\mathbf{G}\|_{2,1}$ can be rewritten as:

$$\|\mathbf{G}\|_{2,1}=\mathrm{Tr}(\mathbf{G}^T\mathbf{UG}),$$

where $\mathbf{U}\in\mathbb{R}^{n\times n}$ is a diagonal matrix with the diagonal elements

$$U_{ii}=\frac{1}{2\|\mathbf{G}_i\|_2}, \quad \text{for} \quad i=1,\ldots,n.$$

In order to find $\mathbf{G}$ and $\mathbf{H}$, we make use of an alternating least squares iterative method in such a way that we will solve (7) with respect to one variable while the other one is taken to be fixed. For this purpose, we first assume that $\mathbf{H}\in\mathbb{R}^{k\times n}$ is fixed. In this respect, it is supposed that

$$\mathcal{L}(\mathbf{G},\mathbf{H})=\|\mathbf{B}-\mathbf{BGH}\|_F^2+\alpha\mathrm{Tr}(\mathbf{G}^T\mathbf{UG}).$$

Now, by taking the partial derivative of $\mathcal{L}$ with respect to $\mathbf{G}$, we have

$$\frac{\partial\mathcal{L}}{\partial\mathbf{G}}=2\mathbf{B}^T\mathbf{BGHH}^T-2\mathbf{B}^T\mathbf{BH}^T+2\alpha\mathbf{UG}.$$

Set $\partial\mathcal{L}/\partial\mathbf{G}=0$. It follows that the matrix $\mathbf{G}$ satisfies Eq. (8).

$$\mathbf{B}^T\mathbf{BGHH}^T+\alpha\mathbf{UG}=\mathbf{B}^T\mathbf{BH}^T. \tag{8}$$

In the same manner, taking the partial derivative of $\mathcal{L}$ with respect to $\mathbf{H}$ when $\mathbf{G}\in\mathbb{R}^{n\times k}$ is assumed to be fixed, we get

$$\frac{\partial\mathcal{L}}{\partial\mathbf{H}}=2\mathbf{G}^T\mathbf{B}^T\mathbf{BGH}-2\mathbf{G}^T\mathbf{B}^T\mathbf{B}.$$

Again, putting $\partial\mathcal{L}/\partial\mathbf{H}=0$, it is obtained that $\mathbf{H}$ satisfies Eq. (9).

$$\mathbf{G}^T\mathbf{B}^T\mathbf{BGH}=\mathbf{G}^T\mathbf{B}^T\mathbf{B}. \tag{9}$$

Algorithm 1 summarizes what have been discussed in this section.

2.3.2 The B-MPMR Method

There are two major drawbacks when data of high-dimension are applied to machine learning methods including a dramatic rise of storage costs and level of redundancy which negatively affect the learning process performance. Inspired by this fact, a set of feature selection techniques have been developed in recent years to produce a solution for these problems. An example of such methods that was successful in representing the original features effectively and reducing the features redundancy is "feature selection based on Maximum Projection and Minimum Redundancy" (MPMR) [38], which can be formed as:

$$\underset{\mathbf{W},\mathbf{H}}{\operatorname{argmin}} \|\mathbf{X}-\mathbf{XWH}\|_F^2+\alpha\mathrm{Tr}(\mathbf{W}^T\mathbf{X}^T\mathbf{XW}\mathbf{1}_k), \quad \text{subject to } \mathbf{W}\geq 0, \mathbf{W}^T\mathbf{W}=\mathbf{E_k}, \tag{10}$$

Algorithm 1 The B-MFFS method.

Input: Data matrix $\mathbf{X} \in \mathbb{R}^{n\times d}$; the regularization parameter α; the number of the selected features k; maximum number of iterations *maxIter*.

1: Initialize the basis of features $B = \{\mathbf{f}_1^b, \mathbf{f}_2^b \ldots, \mathbf{f}_n^b\}$ and consider the matrix $\mathbf{B} = [\mathbf{f}_1^b, \mathbf{f}_2^b \ldots, \mathbf{f}_n^b]$.
2: Initialize $\mathbf{H} \in \mathbb{R}^{k\times n}$.
3: **while** iteration $\leq$ *maxIter* **do**
4: Fix $\mathbf{H}$ and solve $\mathbf{B}^T\mathbf{B}\mathbf{G}\mathbf{H}\mathbf{H}^T + \alpha\mathbf{U}\mathbf{G} = \mathbf{B}^T\mathbf{B}\mathbf{H}^T$ for $\mathbf{G}$.
5: Fix $\mathbf{G}$ and solve $\mathbf{G}^T\mathbf{B}^T\mathbf{B}\mathbf{G}\mathbf{H} = \mathbf{G}^T\mathbf{B}^T\mathbf{B}$ for $\mathbf{H}$.
6: **end while**

Output: Select the k features from $\{\mathbf{f}_1^b, \mathbf{f}_2^b \ldots, \mathbf{f}_n^b\}$ corresponding to the k rows of $\mathbf{G}$ with the largest norms.

in which α is considered to achieve a proper trade-off between the redundancy rate and the approximation degree.

The current section introduces B-MPMR as an improvement of MPMR. The key idea in B-MPMR is to investigate that to what extent the features in a subset of the basis are independent of each other. Suppose that the basis $\mathbf{B} = [\mathbf{f}_1^b, \mathbf{f}_2^b \ldots, \mathbf{f}_n^b] \in \mathbb{R}^{n\times n}$ is as the one mentioned in Section 2.3.1. The B-MPMR technique addresses the redundancy problem by computing the rate of redundancy for each feature in the given feature subset and using the results to guide the process of selecting the features.

Given a subset of features, $\mathbf{X}_I$, there is a representation $\mathbf{X}_I = \mathbf{B}\mathbf{G}$ similar to the one described in Section 2.3.1. For $\mathbf{X}_I$, the rate of redundancy, $\mathrm{red}(I)$, is calculated by Eq. (11).

$$\mathrm{red}(I) = \frac{1}{k^2}\sum_{p=1}^{k}\sum_{q=1}^{k}\mathbf{x}_{i_p}^T\mathbf{x}_{i_q} = \frac{1}{k^2}\mathrm{Tr}(\mathbf{X}_I^T\mathbf{X}_I\mathbf{1}_k) = \frac{1}{k^2}\mathrm{Tr}(\mathbf{G}^T\mathbf{B}^T\mathbf{B}\mathbf{G}\mathbf{1}_k), \tag{11}$$

in which the matrix $\mathbf{1}_k \in \mathbb{R}^{k\times k}$ is defined so that all its entries are one.

We have

$$\mathrm{Tr}(\mathbf{G}^T\mathbf{B}^T\mathbf{B}\mathbf{G}\mathbf{1}_k) = \tilde{\mathbf{1}}_k^T\mathbf{G}^T\mathbf{B}^T\mathbf{B}\mathbf{G}\tilde{\mathbf{1}}_k, \tag{12}$$

in which the vector $\tilde{\mathbf{1}}_k \in \mathbb{R}^k$ whose entries are all one. Considering the fact that $\mathbf{G}^T\mathbf{B}^T\mathbf{B}\mathbf{G}$ is a symmetric positive semi-definite the matrix, it is deduced from Eq. (12) that $\mathrm{Tr}(\mathbf{G}^T\mathbf{B}^T\mathbf{B}\mathbf{G}\mathbf{1}_k) \geq 0$.

Regarding the redundancy problem discussed above, the feature selection problem of the B-MPMR method is formulated as follows:

$$\underset{\mathbf{G}\in\mathbb{R}^{n\times k},\mathbf{H}\in\mathbb{R}^{k\times n}}{\mathrm{argmin}} \|\mathbf{B} - \mathbf{B}\mathbf{G}\mathbf{H}\|_F^2 + \alpha\mathrm{Tr}(\mathbf{G}^T\mathbf{B}^T\mathbf{B}\mathbf{G}\mathbf{1}_k) + \beta\|\mathbf{G}\|_{2,1}, \tag{13}$$

where α and β are two regularization parameters, and the $L_{2,1}$–norm is imposed on the feature selection matrix to assure the sparsity of this matrix.

To find $\mathbf{G}$ and $\mathbf{H}$, the least squares method is employed again to solve (13) with respect to one variable while the other one is fixed. First, assume that $\mathbf{H} \in \mathbb{R}^{k\times n}$ is fixed. We define

$$\mathcal{L}(\mathbf{G}, \mathbf{H}) = \|\mathbf{B} - \mathbf{B}\mathbf{G}\mathbf{H}\|_F^2 + \alpha\mathrm{Tr}(\mathbf{G}^T\mathbf{B}^T\mathbf{B}\mathbf{G}\mathbf{1}_k) + \beta\mathrm{Tr}(\mathbf{G}^T\mathbf{U}\mathbf{G}),$$

where $\mathbf{U} \in \mathbb{R}^{n\times n}$ is a diagonal matrix with the diagonal elements $\mathbf{U}_{ii} = \frac{1}{2\|\mathbf{G}_i\|_2}$ for $i = 1, \ldots, n$.

Now, by taking the partial derivative of $\mathcal{L}$ with respect to $\mathbf{G}$, we have

$$\frac{\partial\mathcal{L}}{\partial\mathbf{G}} = 2\mathbf{B}^T\mathbf{B}\mathbf{G}\mathbf{H}\mathbf{H}^T - 2\mathbf{B}^T\mathbf{B}\mathbf{H}^T + 2\alpha\mathbf{B}^T\mathbf{B}\mathbf{G}\mathbf{1}_k + 2\beta\mathbf{U}\mathbf{G}.$$

Next, assuming that $\partial\mathcal{L}/\partial\mathbf{G} = 0$, we get

$$\mathbf{B}^T\mathbf{B}\mathbf{G}\mathbf{H}\mathbf{H}^T + \alpha\mathbf{B}^T\mathbf{B}\mathbf{G}\mathbf{1}_k + \beta\mathbf{U}\mathbf{G} = \mathbf{B}^T\mathbf{B}\mathbf{H}^T,$$

which can be expressed as

$$\mathbf{B}^T\mathbf{B}\mathbf{G}(\mathbf{H}\mathbf{H}^T + \alpha\mathbf{1}_k) + \beta\mathbf{U}\mathbf{G} = \mathbf{B}^T\mathbf{B}\mathbf{H}^T. \tag{14}$$

In the same manner, assuming that $\mathbf{G} \in \mathbb{R}^{n\times k}$ is fixed and taking the partial derivative of $\mathcal{L}$ with respect to $\mathbf{H}$, we have

$$\frac{\partial\mathcal{L}}{\partial\mathbf{H}} = 2\mathbf{G}^T\mathbf{B}^T\mathbf{B}\mathbf{G}\mathbf{H} - 2\mathbf{G}^T\mathbf{B}^T\mathbf{B}.$$

Setting $\partial\mathcal{L}/\partial\mathbf{H} = 0$, it follows that the matrix $\mathbf{H}$ satisfies Eq. (15).

$$\mathbf{G}^T\mathbf{B}^T\mathbf{B}\mathbf{G}\mathbf{H} = \mathbf{G}^T\mathbf{B}^T\mathbf{B}. \tag{15}$$

Algorithm 2 describes the steps of B-MRPR in brief.

Algorithm 2 The B-MPMR method.

Input: Data matrix $\mathbf{X} \in \mathbb{R}^{n\times d}$; the regularization parameters α and β; the number of the selected features k; the maximum number of iterations *maxIter*.

1: Initialize the basis of features $B = \{\mathbf{f}_1^b, \mathbf{f}_2^b \ldots, \mathbf{f}_n^b\}$ and consider the matrix $\mathbf{B} = [\mathbf{f}_1^b, \mathbf{f}_2^b \ldots, \mathbf{f}_n^b]$.
2: Initialize $\mathbf{H} \in \mathbb{R}^{k\times n}$.
3: **while** iteration $\leq$ *maxIter* **do**
4: Fix $\mathbf{H}$ and solve the matrix equation $\mathbf{B}^T\mathbf{B}\mathbf{G}(\mathbf{H}\mathbf{H}^T + \alpha\mathbf{1}_k) + \beta\mathbf{U}\mathbf{G} = \mathbf{B}^T\mathbf{B}\mathbf{H}^T$ for $\mathbf{G}$.
5: Fix $\mathbf{G}$ and solve the matrix equation $\mathbf{G}^T\mathbf{B}^T\mathbf{B}\mathbf{G}\mathbf{H} = \mathbf{G}^T\mathbf{B}^T\mathbf{B}$ for $\mathbf{H}$.
6: **end while**

Output: Select the k features from $\{\mathbf{f}_1^b, \mathbf{f}_2^b \ldots, \mathbf{f}_n^b\}$ corresponding to the k rows of $\mathbf{G}$ with the largest norms.

2.3.3 The B-SGFS Method

The majority of former techniques consider the original space of features as the domain on which the feature selection process is carried out as well as making assumption that there is a smooth manifold on which the original data are distributed [44, 45, 46]. For instance, the Subspace learning-based Graph regularized Feature Selection (SGFS) method [39] has been recently developed by including the notion of graph regularization in the objective function of a former feature selection method. This technique is formulated as:

$$\underset{\mathbf{W},\mathbf{H}}{\operatorname{argmin}}\, \alpha\|\mathbf{X}-\mathbf{X}\mathbf{W}\mathbf{H}\|_F^2 + \operatorname{Tr}(\mathbf{H}\mathbf{L}\mathbf{H}^T) + \beta\|\mathbf{W}\|_{2,1}, \quad \text{subject to } \mathbf{W}^T\mathbf{W} = \mathbf{E}_k, \mathbf{H} \geq 0, \mathbf{W} \geq 0, \tag{16}$$

in which α and β are nonnegative balance parameters, and $\mathbf{L} \in \mathbb{R}^{d\times d}$ is the feature Laplacian matrix. In Eq. (16), the term $\operatorname{Tr}(\mathbf{H}\mathbf{L}\mathbf{H}^T)$ handles the geometric structure preservation task for the feature manifold. Moreover, to guarantee that the matrix of feature selection is sparse, this matrix is constrained by the $L_{2,1}$–norm in the objective function of SGFS.

In this section, the B-SGFS method is offered as a technique to select the most discriminative features from a basis of the original feature space and to preserve the geometric structure of features

associated with the basis manifold. This method is different from the SGFS method in terms of two properties including geometric structure preservation and feature manifold reduction. To be more precise, the main idea of our proposed B-SGFS method is to reduce the original feature graph through introducing a basis for the original feature space within which the selected feature subset is chosen. In other words, the reduced graph includes only the elements of the basis determined by the suggested method as its vertices. Therefore, instead of the original feature graph, the reduced graph can be applied as a model of the feature manifold. From a geometric point of view, this issue can be interpreted as follows. The manifold of features is represented by one of its sub-manifolds. This sub-manifold is determined by the basis that the proposed method introduces and it is composed of all the features included in that basis. In fact, considering only the sub-manifold associated with a basis of features allows us to access the information about the whole feature manifold as well.

Let $\mathbf{B} = [\mathbf{f}_1^b, \mathbf{f}_2^b, \ldots, \mathbf{f}_n^b] \in \mathbb{R}^{n\times n}$ be a basis of features. Assuming that the basis of features exists on a sub-manifold of the original manifold of features, the similarity of the ith and the jth basis features for $i, j \in \{1, 2, \ldots, n\}$, is denoted by $\mathbf{S}_{ij}^b$ and is defined as:

$$\mathbf{S}_{ij}^b = \begin{cases} e^{\frac{-\|\mathbf{f}_i^b - \mathbf{f}_j^b\|_2^2}{\sigma}} & \text{if } \mathbf{f}_i^b \in N(\mathbf{f}_j^b) \text{ or } \mathbf{f}_j^b \in N(\mathbf{f}_i^b) \\ 0 & \text{otherwise} \end{cases}, \tag{17}$$

where the set $N(\mathbf{f}_i^b)$ is the k-nearest neighbor corresponding to $\mathbf{f}_i^b$, and σ denotes the Gaussian parameter. In addition, the feature Laplacian matrix $\mathbf{L}^b$ corresponding to the basis of features is defined as $\mathbf{L}^b = \mathbf{D}^b - \mathbf{S}^b$ in which $\mathbf{D}^b$ is an $n \times n$ diagonal matrix with the diagonal entries $\mathbf{D}_{ii}^b = \sum_{j=1}^n \mathbf{S}_{ij}^b$.

Suppose that the coefficient matrix is $\mathbf{H} = [\mathbf{h}_1, \mathbf{h}_2, \ldots, \mathbf{h}_n]$. The problem regarding the preservation of the geometric structure of features associated with the basis manifold is presented as:

$$\mathrm{Tr}(\mathbf{H}\mathbf{L}^b\mathbf{H}^T) = \frac{1}{2}\sum_{i=1}^{n}\sum_{j=1}^{n} \|\mathbf{h}_i - \mathbf{h}_j\|_2^2 \mathbf{S}_{ij}^b. \tag{18}$$

Considering Eq. (18), in case the level of the similarity between the ith and the jth features in the basis is sufficiently high, the similarity between the vectors $\mathbf{h}_i$ and $\mathbf{h}_j$ are also considerably strong. That is to say that the similarity of the feature vectors in the original manifold implies the similarity of the corresponding vectors in the sub-manifold determined by the basis. In brief, this representation leads to a substantial reduction of the feature manifold so that the local geometry of features is preserved while the size of the graph is enormously reduced. This issue enhances the performance of our method and reduces the computational costs to a considerable extent.

Now, considering the ultimate goal of an unsupervised feature selection to search a low-dimensional feature subset that best characterizes the original feature space, we define the optimization framework of the proposed method B-SGFS as follows:

$$\underset{\mathbf{G}\in\mathbb{R}^{n\times k}, \mathbf{H}\in\mathbb{R}^{k\times n}}{\mathrm{argmin}} \|\mathbf{B} - \mathbf{B}\mathbf{G}\mathbf{H}\|_F^2 + \alpha\mathrm{Tr}(\mathbf{H}\mathbf{L}^b\mathbf{H}^T) + \beta\|\mathbf{G}\|_{2,1}, \tag{19}$$

in which α and β are two regularization parameters, and the following principle fact has been utilized in (19): every feature subset of X can be expressed uniquely as a linear combination of the features associated with the basis B, and as an immediate consequence, it is deduced that there is a matrix $\mathbf{G} \in \mathbb{R}^{n\times k}$ such that $\mathbf{X}_I = \mathbf{B}\mathbf{G}$.

In order to find $\mathbf{G}$ and $\mathbf{H}$, we make use of an alternating least squares iterative method in such a way that we will solve (19) with respect to one variable while the other variable is assumed to be fixed. For this purpose, first, let $\mathbf{H} \in \mathbb{R}^{k\times n}$ is taken to be fixed and suppose that

$$\mathcal{L}(\mathbf{G}, \mathbf{H}) = \|\mathbf{B} - \mathbf{BGH}\|_F^2 + \alpha \mathrm{Tr}(\mathbf{HL}^b\mathbf{H}^T) + \beta \mathrm{Tr}(\mathbf{G}^T\mathbf{UG}),$$

where $\mathbf{U} \in \mathbb{R}^{n\times n}$ is a diagonal matrix with the diagonal elements $\mathbf{U}_{ii} = \frac{1}{2\|\mathbf{G}_i\|_2}$ for $i = 1, \ldots, n$.

Now, by taking the partial derivative of $\mathcal{L}$ with respect to $\mathbf{G}$, we get

$$\frac{\partial \mathcal{L}}{\partial \mathbf{G}} = 2(\mathbf{B}^T\mathbf{BGHH}^T - \mathbf{B}^T\mathbf{BH}^T) + 2\beta\mathbf{UG}.$$

Next, we assume that $\partial\mathcal{L}/\partial\mathbf{G} = 0$. It follows that the matrix $\mathbf{G}$ satisfies Eq. (20).

$$\mathbf{B}^T\mathbf{BGHH}^T + \beta\mathbf{UG} = \mathbf{B}^T\mathbf{BH}^T. \tag{20}$$

In the same manner, we assume that $\mathbf{G} \in \mathbb{R}^{n\times k}$ is fixed and taking the partial derivative of $\mathcal{L}$ with respect to $\mathbf{H}$, we have

$$\frac{\partial \mathcal{L}}{\partial \mathbf{H}} = 2(\mathbf{G}^T\mathbf{B}^T\mathbf{BGH} - \mathbf{G}^T\mathbf{B}^T\mathbf{B}) + 2\alpha\mathbf{HL}^b.$$

Now, suppose that $\partial\mathcal{L}/\partial\mathbf{H} = 0$. It results that the matrix $\mathbf{H}$ satisfies Eq. (21).

$$\mathbf{G}^T\mathbf{B}^T\mathbf{BGH} + \alpha\mathbf{HL}^b = \mathbf{G}^T\mathbf{B}^T\mathbf{B}. \tag{21}$$

Algorithm 3 presents a summary of what discussed in this section.

Algorithm 3 The B-SGFS method.

Input: Data matrix $\mathbf{X} \in \mathbb{R}^{n\times d}$; the regularization parameters α and β; the number of the selected features k; the maximum number of iterations *maxIter*.

1: Initialize the basis of features $B = \{\mathbf{f}_1^b, \mathbf{f}_2^b \ldots, \mathbf{f}_n^b\}$ and consider the matrix $\mathbf{B} = [\mathbf{f}_1^b, \mathbf{f}_2^b \ldots, \mathbf{f}_n^b]$.
2: Compute the feature Laplacian matrix $\mathbf{L}^b$ corresponding to the basis of features.
3: Initialize $\mathbf{H} \in \mathbb{R}^{k\times n}$.
4: Initialize the diagonal matrix $\mathbf{U} \in \mathbb{R}^{n\times n}$.
5: **while** iteration $\leq$ *maxIter* **do**
6: Fix $\mathbf{H}$ and solve the matrix equation $\mathbf{B}^T\mathbf{BGHH}^T + \beta\mathbf{UG} = \mathbf{B}^T\mathbf{BH}^T$ for $\mathbf{G}$.
7: Fix $\mathbf{G}$ and solve the matrix equation $\mathbf{G}^T\mathbf{B}^T\mathbf{BGH} + \alpha\mathbf{HL} = \mathbf{G}^T\mathbf{B}^T\mathbf{B}$ for $\mathbf{H}$.
8: Update the diagonal matrix $\mathbf{U}$ according to the rule $\mathbf{U}_{ii} = \frac{1}{2\|\mathbf{G}_i\|_2}$, where $i = 1, \ldots, n$.
9: **end while**

Output: Select the k features of $\{\mathbf{f}_1^b, \mathbf{f}_2^b \ldots, \mathbf{f}_n^b\}$ relating to the k rows of $\mathbf{G}$ with the largest norms.

2.4 Solving the Matrix Equations in B-MFFS, B-MPMR and B-SGFS

As it was discussed in the previous sections, the following matrix equations have been derived for the three proposed methods B-MFFS, B-MPMR and B-SGFS.

$$\textbf{B-MFFS:} \quad \begin{cases} \text{To obtain } \mathbf{G}\text{:} & \mathbf{B}^T\mathbf{B}\mathbf{G}\mathbf{H}\mathbf{H}^T + \alpha\mathbf{U}\mathbf{G} = \mathbf{B}^T\mathbf{B}\mathbf{H}^T. \\ \text{To obtain } \mathbf{H}\text{:} & \mathbf{G}^T\mathbf{B}^T\mathbf{B}\mathbf{G}\mathbf{H} = \mathbf{G}^T\mathbf{B}^T\mathbf{B}. \end{cases}$$

$$\textbf{B-MPMR:} \quad \begin{cases} \text{To obtain } \mathbf{G}\text{:} & \mathbf{B}^T\mathbf{B}\mathbf{G}(\mathbf{H}\mathbf{H}^T + \alpha\mathbf{1}_k) + \beta\mathbf{U}\mathbf{G} = \mathbf{B}^T\mathbf{B}\mathbf{H}^T. \\ \text{To obtain } \mathbf{H}\text{:} & \mathbf{G}^T\mathbf{B}^T\mathbf{B}\mathbf{G}\mathbf{H} = \mathbf{G}^T\mathbf{B}^T\mathbf{B}. \end{cases}$$

$$\textbf{B-SGFS:} \quad \begin{cases} \text{To obtain } \mathbf{G}\text{:} & \mathbf{B}^T\mathbf{B}\mathbf{G}\mathbf{H}\mathbf{H}^T + \beta\mathbf{U}\mathbf{G} = \mathbf{B}^T\mathbf{B}\mathbf{H}^T. \\ \text{To obtain } \mathbf{H}\text{:} & \mathbf{G}^T\mathbf{B}^T\mathbf{B}\mathbf{G}\mathbf{H} + \alpha\mathbf{H}\mathbf{L} = \mathbf{G}^T\mathbf{B}^T\mathbf{B}. \end{cases}$$

Since the coefficient matrices described in the above matrix equations are symmetric positive semi-definite, according to the results mentioned in [47], we can employ some reliable techniques such as the global conjugate gradient method to solve such matrix equations. In Appendix A, the details of the global conjugate gradient method will be explained. For more information about the conjugate gradient method as well as the global version of this method, see [47, 48, 49] and references therein.

2.5 An Algorithm to Build a Basis for the Features Space

In this section, we aim to describe how to find a proper basis for feature space. The technique of Variance Score (VS) is an effective method that determines a discriminative feature as the one whose VS is a large value. This technique is very simple to implement and is commonly used for feature selection problems in unsupervised mode. It is known as a fact that the variance of data represents the level of its spread over a given domain, and variance maximization for the data that are reduced and transformed into a lower dimension leads to far more information extraction. Considering the remarkable ability of this method, our proposed techniques apply it to determine which features are the most discriminative to be included in the basis we are going to form. Such a basis is constructed as follows. First, computing every feature's VS, the features are reordered in terms of their VS so that the feature with the highest VS comes first, and the other features ordered in a designing manner after it. Next, the first feature, the one whose VS is the highest value, is considered as the first feature of the basis and the set including this single feature is extended to a basis of features by applying the extension algorithm to the other features ordered after it. Algorithm 4 provides a detailed description of this process. For a detailed review of the extension method for construction of a basis, see Appendix B.

3 Computational Experimental Results

To validate the three proposed methods, B-MFFS, B-MPMR and B-SGFS, in terms of their performance, some experiments are conducted in this section on a number of well-known biological datasets. To analyze the results, two essential metrics are used. First, these metrics are described in brief. Following this, the results of the experiments regarding the efficiency and efficacy of the proposed techniques are discussed.

Algorithm 4 Building a basis for the feature space.

Input: Data matrix $\mathbf{X} = [\mathbf{f}_1, \mathbf{f}_2, \ldots, \mathbf{f}_d] \in \mathbb{R}^{n \times d}$ in which $1 < \text{rank}(\mathbf{X}) = p \leq \min\{n, d\}$.
Output: A basis B for the vector space spanned by the set $\{\mathbf{f}_1, \mathbf{f}_2, \ldots, \mathbf{f}_d\}$ of the features.

for $i = 1$ to d **do**
  $\text{VS}(i) \longleftarrow$ Variance Score (VS) for the ith feature.
end for
Arranging the VSs in a descending order.
$\mathbf{X}^{\text{new}} \longleftarrow$ Rearranging the features in $\mathbf{X}$ in terms of the order of their corresponding VS. Set $\mathbf{X}^{\text{new}} = [\mathbf{f}_1^{\text{new}}, \mathbf{f}_2^{\text{new}}, \ldots, \mathbf{f}_d^{\text{new}}]$.
Set $B = \{\mathbf{f}_1^{\text{new}}\}$.
for $k = 2 : d$ **do** // The basis extension technique
  if $\mathbf{f}_k^{\text{new}} \notin \text{span}(B)$ **then**
    $B \leftarrow B \cup \{\mathbf{f}_k^{\text{new}}\}$.
  end if
  if $|B| = p$ **then**
    Stop.
  end if
end for

3.1 Datasets

In this paper, to evaluate the proposed methods, eight cancer gene expression datasets are used. A description of these datasets are presented in Table 1.

Table 1: The information of eight datasets utilized in the computational experiments.

Dataset	Abbreviation	# Samples	# Features	# Classes	Reference
Embryonal Tumors of CNS	CNS	60	7129	2	[50]
Colon Cancer	Colon	62	2000	2	[51]
Diffuse Large B-cell Lymphomas	DLBCL	47	4026	2	[52]
Glioblastoma Multiforme	GBM	85	22283	2	[53]
TOX-171	TOX-171	171	5748	4	[28]
Lung Cancer	Lung	73	325	7	[54]
Prostate Cancer	Prostate	102	5966	2	[54]
Cancer Cell Line Encyclopedia	CCLE	343	1900	2	[55]

3.2 Computational Experimental Setting

Before performing the experiments, the parameters included in the methods are set as follows. For all methods, the tuning of the regular parameters is carried out making use of a grid-search. This issue is a leading factor in drawing reasonable and fair comparisons. This way, we set $\alpha = 1$ in MPMR and $\rho = 10^8$ in MPMR and MFFS [37, 38]. In addition, the search domain is selected as $\{10^i |\ i = -8, -7, \ldots, 7, 8\}$ for the rest of the balancing parameters in all methods. Moreover, for all methods, the maximum number of iterations and the number of the selected features from each dataset are set to 30 and $\{10, 20, 30, \ldots, 100\}$, respectively. For methods that preserve the geometric structure of features, $\{10^i |\ i = 0, 1, \ldots, 5\}$ is considered as the search domain for σ, and each neighbor size is selected to be 5 on each dataset. Employing the k-means technique, the performance of the process of

clustering is examined subject to the selected features, where for a given dataset, the true number of the classes is denoted by c. Furthermore, initializing each parameter at random, the clustering algorithm is repeated 20 times, and the averaging the result of these iterations, the best outcome is reported.

3.3 Evaluation Metrics for Comparison

In order to carry out proper evaluation of the proposed and benchmark algorithms, two commonly used performance evaluation metrics for unsupervised methods, including Clustering Accuracy (ACC) and Normalized Mutual Information (NMI), are employed. Notice that a greater value of ACC/NMI corresponding to a method indicates that the method under consideration achieves a better performance. The metric ACC is formulated by Eq. (22).

$$\mathrm{ACC} = \frac{1}{k}\sum_{j=1}^{k}\delta(d_j, \mathrm{map}(e_j)), \tag{22}$$

in which k denotes the total number of samples, d_j and e_j symbolize respectively the ground truth label for the sample x_i and the clustering label, $\mathrm{map}(.)$ represents an optimal mapping function that handles the task of matching the labels predicted by the given feature selection method to the real ones, and the indicator function $\delta(a, b)$ is defined by Eq. (23).

$$\delta(a, b) = \begin{cases} 1 & ; \quad \text{if } a = b \\ 0 & ; \quad \text{otherwise} \end{cases}. \tag{23}$$

Let W and Z be random variables. The metric NMI is given by Eq. (24).

$$\mathrm{NMI}(W, Z) = \frac{\mathrm{I}(W, Z)}{\sqrt{\mathrm{H}(W)\mathrm{H}(Z)}}, \tag{24}$$

where $\mathrm{I}(W, Z)$ indicates the mutual information between W and Z, and $\mathrm{H}(.)$ is the entropy function.

3.4 Methods and Modalities

To conduct the experiments, we make comparisons between the proposed techniques and a number of benchmark methods including the Baseline, Variance Score (VS) [56], Laplacian Score (LS) [57], MFFS [37], MPMR [38] and SGFS [39]. In Baseline, all original features are used. Variance Score computes every feature's variance, and determines the optimal features as the ones whose variance is the largest compared to the other features. In Laplacian Score, the intrinsic geometry of data is taken into consideration. The last three methods, MFFS, MPMR and SGFS, were also described in Subsection 2.3.

3.5 Results and Discussion

In order to draw comparisons of the proposed methods with other techniques, six various state-of-the-art methods were examined in terms of their performance on seven benchmark datasets. To this aim, ACC and NMI were computed for the selected methods. The results of these experiments are presented in Tables 2 and 3 in which the first and the second best results are marked in boldface and are underlined, respectively.

According to Table 2, on all the datasets, the first and the second best values of ACC were achieved by the three proposed methods, B-SGFS, B-MPMR and B-MFFS. In addition, B-MFFS outperformed all the conventional methods in terms of ACC. With the exception of the ACC value for MPMR which equals that value for B-MPMR on DLBCL, B-MPMR gave a better performance compared to the conventional methods. It is also clear that B-SGFS showed a better performance compared to the state-of-the-art methods except for SGFS on CNS. In this case the difference between the ACC value of the two methods is very small. A key aspect of the proposed methods is the lower number of the selected features compared to that number corresponding to the conventional methods. It is clear from Table 2 that this number, presented in parentheses, is far smaller for our three methods than that number for the other methods in most cases which is a big advantage. Figure 2 illustrates the bar chart of ACC values for all the methods indicated in Table 2 on the seven benchmark datasets presented in Table 1. The blue, black and red bars that correspond to B-SGFS, B-MPMR and B-MFFS, respectively, show the superiority of our proposed methods over all the other ones except for two mentioned cases.

Table 2: Clustering accuracy (ACC±STD%) results for different feature selection methods on seven datasets. The numbers in parentheses are the numbers of selected features corresponding to the best clustering results. The best results in each row are highlighted in bold and the second best results are underlined. Note that the higher ACC values are, the better the clustering performance is.

Dataset	Baseline	VS	LS	MFFS	MPMR	SGFS	B-MFFS	B-MPMR	B-SGFS
CNS	53.33 ± 1.45	56.66 ± 0.04 (70)	58.66 ± 1.02 (80)	61.75 ± 2.78 (50)	61.66 ± 0.00 (70)	63.12 ± 0.00 (60)	62.33 ± 2.05 (10)	63.25 ± 0.37 (10)	**64.25 ± 3.35** (20)
Colon	78.54 ± 6.95	58.06 ± 1.14 (20)	60.00 ± 9.38 (90)	74.19 ± 0.29 (10)	74.21 ± 2.91 (90)	77.41 ± 1.45 (40)	80.64 ± 0.03 (10)	84.91 ± 2.52 (10)	**85.48 ± 0.00** (10)
DLBCL	59.57 ± 1.23	65.95 ± 0.01 (10)	57.44 ± 0.72 (40)	85.10 ± 0.14 (40)	87.23 ± 0.14 (70)	80.85 ± 0.43 (40)	**95.74 ± 0.29** (10)	87.23 ± 0.29 (10)	90.85 ± 2.85 (10)
GBM	67.05 ± 0.01	68.23 ± 0.00 (40)	69.41 ± 0.00 (10)	70.58 ± 0.00 (20)	70.58 ± 0.00 (10)	72.23 ± 0.00 (50)	75.29 ± 0.00 (10)	75.29 ± 1.45 (10)	**76.47 ± 0.26** (10)
TOX-171	41.25 ± 0.72	42.13 ± 0.99 (20)	40.35 ± 0.72 (10)	42.13 ± 0.13 (90)	41.49 ± 1.65 (60)	38.26 ± 0.87 (100)	**45.08 ± 0.54** (10)	44.82 ± 0.91 (40)	44.44 ± 0.72 (20)
Lung	76.78 ± 5.03	59.58 ± 5.68 (100)	65.82 ± 3.72 (100)	77.80 ± 4.6130 (30)	79.58 ± 6.57 (100)	80.75 ± 5.45 (90)	81.16 ± 4.96 (50)	**82.46 ± 5.83** (50)	82.05 ± 6.91 (50)
Prostate	57.84 ± 0.00	65.68 ± 0.06 (10)	60.78 ± 0.01 (10)	61.76 ± 0.00 (50)	62.84 ± 1.38 (60)	63.72 ± 1.45 (10)	69.60 ± 0.02 (10)	**69.72 ± 0.01** (10)	67.64 ± 0.00 (10)

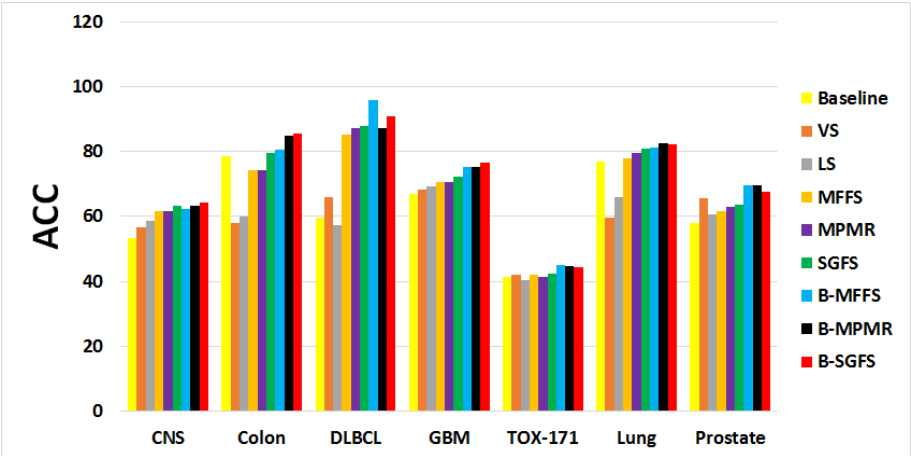

Figure 2: The average results of the ACC metric on seven datasets. The x-axis indicates the different datasets, and the y-axis represents the values of the ACC results obtained for each feature selection method. Note that the higher ACC values are, the better the clustering performance is.

Table 3: Normalized mutual information (NMI±STD%) results for different feature selection methods on seven datasets. The numbers in parentheses are the numbers of selected features corresponding to the best clustering results. The best results in each row are highlighted in bold and the second best results are underlined. Note that the higher NMI values are, the better the clustering performance is.

Dataset	Baseline	VS	LS	MFFS	MPMR	SGFS	B-MFFS	B-MPMR	B-SGFS
CNS	1.17 ± 0.00	2.25 ± 0.45 (70)	2.44 ± 0.45 (90)	2.93 ± 0.45 (100)	1.60 ± 0.80 (30)	$\mathbf{8.79 \pm 0.00}$ (30)	3.91 ± 0.59 (10)	3.61 ± 0.31 (30)	$\underline{4.26 \pm 0.31}$ (20)
Colon	27.35 ± 9.96	2.96 ± 1.63 (10)	7.27 ± 1.23 (100)	24.30 ± 0.14 (100)	21.08 ± 0.54 (40)	30.03 ± 0.00 (10)	33.03 ± 0.01 (10)	$\underline{36.67 \pm 5.43}$ (10)	$\mathbf{37.89 \pm 1.82}$ (10)
DLBCL	2.93 ± 1.09	7.46 ± 1.13 (10)	2.04 ± 0.45 (40)	39.45 ± 0.00 (40)	48.46 ± 0.72 (70)	30.54 ± 0.72 (40)	$\mathbf{78.80 \pm 0.00}$ (10)	48.46 ± 0.07 (10)	$\underline{58.06 \pm 6.04}$ (10)
GBM	21.74 ± 0.03	6.61 ± 1.82 (40)	5.52 ± 2.75 (60)	7.10 ± 0.18 (30)	7.10 ± 0.82 (10)	8.75 ± 0.00 (60)	23.91 ± 0.36 (10)	$\underline{25.28 \pm 1.09}$ (10)	$\mathbf{31.61 \pm 0.27}$ (10)
TOX-171	13.54 ± 0.23	12.27 ± 0.65 (20)	11.68 ± 1.97 (90)	12.82 ± 1.52 (80)	16.22 ± 1.89 (60)	10.41 ± 1.02 (100)	$\underline{17.39 \pm 0.89}$ (50)	16.83 ± 1.03 (10)	$\mathbf{18.51 \pm 0.01}$ (20)
Lung	73.13 ± 2.52	56.36 ± 3.32 (100)	62.85 ± 2.16 (100)	73.22 ± 4.43 (60)	73.67 ± 4.49 (100)	75.61 ± 4.38 (100)	76.41 ± 3.61 (50)	$\underline{77.29 \pm 4.50}$ (50)	$\mathbf{79.01 \pm 5.33}$ (50)
Prostate	1.85 ± 0.03	7.25 ± 0.00 (10)	5.28 ± 0.06 (10)	5.29 ± 0.03 (50)	7.74 ± 1.28 (60)	7.45 ± 0.91 (10)	$\underline{13.43 \pm 0.79}$ (10)	$\mathbf{16.03 \pm 0.27}$ (10)	10.21 ± 0.22 (10)

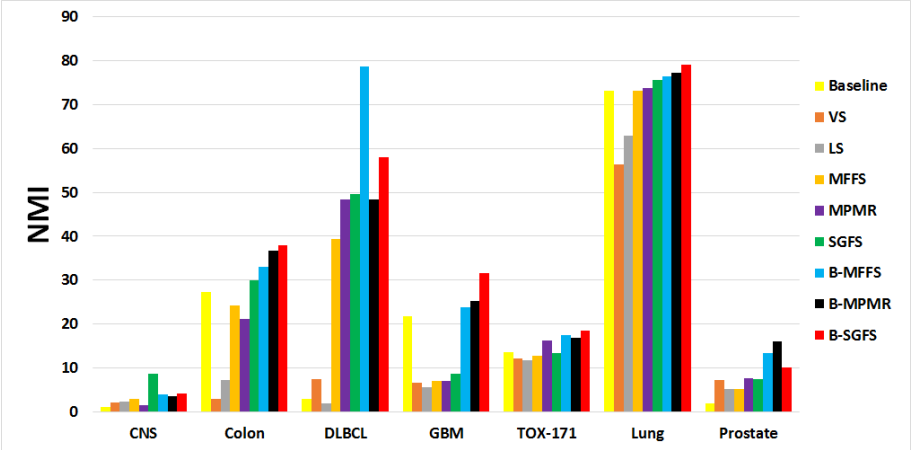

Figure 3: The average results of the NMI metric on seven datasets. The x-axis indicates the different datasets, and the y-axis represents the values of the NMI results obtained for each feature selection method. Note that the higher NMI values are, the better the clustering performance is.

Moving to Table 3, it is clear that B-MFFS, B-MPMR and B-SGFS are infinitely preferable in terms of NMI than the conventional methods on all the datasets used in this paper with the exception of two cases. The first exception occurred for SGFS on CNS, where this algorithm performed better compared with all our three methods, and the second one was raised on DLBCL in which the values of NMI for B-MPMR and MPMR were equal. In all the other cases, the first and second best results were obtained by the proposed methods. Again, the number of the selected features can be considered as an outstanding achievement of our methods since in almost all cases, these algorithms selected lower number of the features in compared to the conventional methods. In Figure 3, the bar chart of the values of NMI corresponding to the proposed and conventional methods on the seven benchmark datasets are shown. It can be seen from Figure 3 that B-MFFS, B-MPMR and B-SGFS, illustrated by blue, black and red bars, respectively, outperformed the conventional methods with two aforementioned exceptions.

Furthermore, Figure 4 presents the bar charts of both the ACC and NMI values of all the conventional and proposed algorithms averaged over all the benchmark datasets. This figure shows that for

all the three proposed methods, the average values of ACC and NMI, illustrated by the gray and red bars, respectively, are higher than that values corresponding to the conventional methods. This means that overall, the B-MFFS, B-MPMR and B-SGFS algorithms show a stronger performance in terms of ACC and NMI compared to with the benchmark methods.

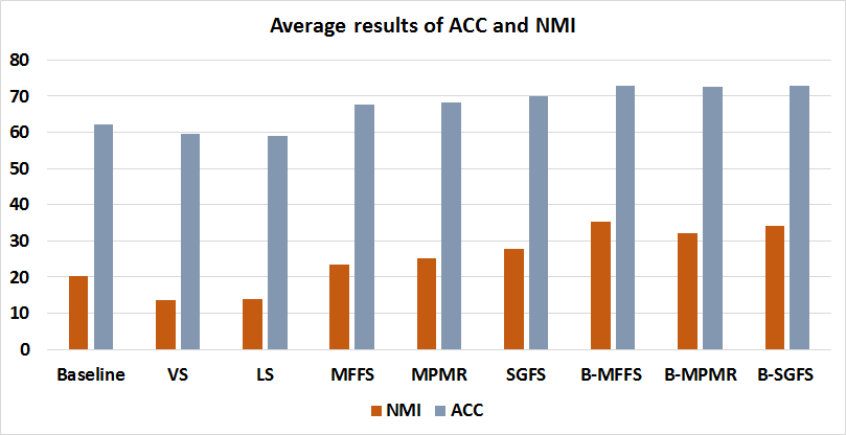

Figure 4: The average values of the metrics ACC and NMI. The x-axis indicates the different feature selection methods, and the y-axis represents the obtained values of the metrics. Note that the higher ACC and NMI values are, the better the clustering performance is.

3.6 Comparison Between MFFS and B-MFFS

The data in Table 2 show that in terms of ACC, B-MFFS outperforms the MFFS on all the datasets. Those data also indicate that B-MFFS stands at the first and second ranks on two datasets, DLBCL and TOX-171, and on the dataset GBM, respectively. In addition, it is apparent from Table 2 that compared to MFFS, B-MFFS selects a lower number of features on all datasets except for Lung, where both numbers are equal. Based on the data given in Table 3, it is clear that B-MFFS is superior in terms of NMI to MFFS on all the datasets and comparing all the considered methods, its results achieves the first and the second ranks respectively on the dataset DLBCL and on the datasets TOX-171 and Lung. Moreover, in terms of NMI, the number of the features selected by B-MFFS is lower than that number corresponding to MFFS. In Figure 5, the bar charts of the values of ACC and NMI, relevant to MFFS and B-MFFS and averaged over all the benchmark datasets, are presented. As Figure 5 shows, the average values of both indices for B-MFFS, represented by blue bars, are greater than that values for B-MFFS, represented by red bars. Thus, the average performance of B-MFFS is better than that of its corresponding conventional method.

3.7 Comparison Between MPMR and B-MPMR

To compare B-MPMR with its corresponding conventional method, the data in Tables 2 and 3 should be considered. It is obvious from these tables that in terms of both ACC and NMI, B-MPMR performs better than the MPMR over all the datasets except for DLBCL over which both the methods have the same performance. Furthermore, compared to all the methods considered in the experiments, B-MPMR stands at the first and the second ranks in terms of ACC respectively on two datasets Lung and Prostate and on the datasets CNS, Colon, GBM and TOX-171. In terms of NMI, B-MPMR also

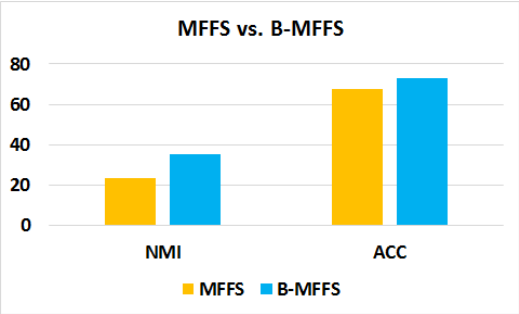

Figure 5: Comparison results of the MFFS and B-MFFS methods in respect of the average values of the metrics ACC and NMI.

achieves the first and second best results on the dataset Prostate and on the datasets Colon, GBM and Lung, respectively. Moreover, it can be seen from Tables 2 and 3 that the number of the features selected by B-MPMR is lower compared to that number for MPMR over all the datasets with three exceptions including GBM in Table 2 and CNS and GBM in Table 3, where both methods selects the same number of features. The bar charts of the ACC and NMI values for MPMR and B-MPMR, averaged over all the benchmark datasets, are depicted in Figure 6. It is apparent from Figure 6 that the overall performance of B-MPMR is stronger in terms of ACC and NMI compared to that of MPMR since for B-MPMR, the ACC and NMI average values, that are illustrated by black bars, are greater compared with that values for MPMR, which are represented by purple bars.

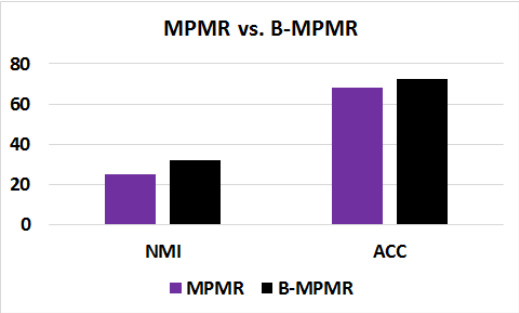

Figure 6: Comparison results of the MPMR and B-MPMR methods in respect of the average values of the metrics ACC and NMI.

3.8 Comparison Between SGFS and B-SGFS

As it can be seen from Tables 2 and 3, the values of ACC and NMI for B-SGFS is better than that of SGFS over all the datasets with the exception of CNS over which the NMI value for SGFS is greater than that of B-SGFS. In addition, compared to all the conventional methods and the two other proposed methods, B-SGFS holds the first and the second ranks in terms of ACC over the datasets CNS, Colon and GBM and over the datasets DLBCL and Lung, respectively. When considering NMI, the first and the second best results of B-SGFS is obtained over the datasets Colon, GBM, TOX-171 and Lung and on the datasets CNS and DLBCL, respectively. Furthermore, B-SGFS selects a smaller number of features in compared to SGFS over all the benchmark datasets except for Prostate in Table 2 and Colon and Prostate in Table 3, where the number of features selected by both methods are the

same. Figure 7 illustrates the bar charts of the ACC and NMI values averaged over all the benchmark datasets corresponding to SGFS and B-SGFS. In this figure, the green bars represent the average value of SGFS and the red bars illustrate that of B-SGFS. From Figure 7, it is clear that B-SGFS achieves a better average performance in terms of ACC and NMI than does SGFS.

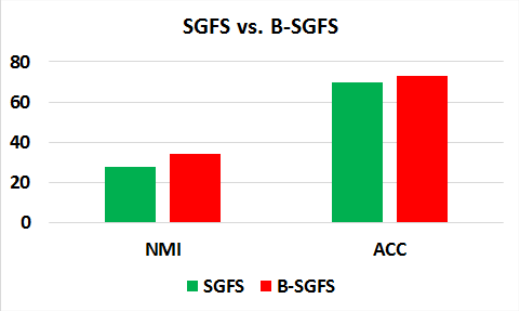

Figure 7: Comparison results of the SGFS and B-SGFS methods in respect of the average values of the metrics ACC and NMI.

3.9 Comparison Among the Proposed Methods

To draw comparisons of the proposed methods with each other, first, we consider their values of ACC in Table 2. Based on these data, B-SGFS holds the first rank on datasets CNS, Colon and GBM. Over CNS and Colon, B-MPMR stands at the second rank and on GBM, both B-MFFS and B-MPMR achieves the second rank simultaneously. The B-MFFS algorithm obtains the best results on the datasets DLBCL and TOX-171. The B-SGFS algorithm stands after it on DLBCL, while the B-MPMR algorithm produces the second best results on TOX-171. Finally, on the datasets Lung and Prostate, B-MPMR stands at the first rank. On Lung, B-SGFS holds the second rand while over Prostate, B-MFFS achieves the second best results. In terms of the number of the selected features, B-MFFS obtains the best results since it selects 10 features over all the benchmark datasets except for Lung over which it selects 50 features that is the same as the number of features the two other proposed methods select on this dataset. The B-MPMR algorithm selects 10 features over the rest of the datasets with the exception of TOX-171 over which it selects 40 features, while B-SGFS selects 20 features on CNS and TOX-171 and 10 feature on the rest of the datasets except for Lung.

Moving to Table 3, the NMI values are considered to make comparisons of our proposed methods. It is clear form this Table that with the exception of CNS on which SGFS produces the best results, for rest of the datasets, our methods obtains the best results. Even on CNS, B-SGFS holds the second best rank. This method also stands at the first rank over four datasets including Colon, GBM, TOX-171 and Lung. The B-MPMR method stands after it over Colon, GBM and Lung, while B-MFFS holds the second rank on TOX-171. The data in Table 3 also indicates that on the dataset Prostate, B-MPMR and B-MFFS achieve the first and the second best results, respectively, while over the dataset DLBCL, B-MFFS and B-SGFS produce respectively the first and the second best outcomes. Moreover, B-MPMR selects 30 and 50 features on CNS and Lung, respectively, and it selects 10 features over the rest of the datasets. In terms of the number of the selected features, B-MPMR perform better than the two other proposed methods. The B-MFFS algorithm selects 50 features on each of TOX-171 and Lung, while it selects 10 features over the rest of the datasets. The number of the features selected by B-SGFS is 20 on each of CNS and TOX-171, 50 on Lung and 10 over the rest of benchmark datasets.

3.10 Methods and Their Running Times

In Figure 8, the bar charts for running time of all the proposed and the conventional methods are illustrated on all the benchmark datasets.

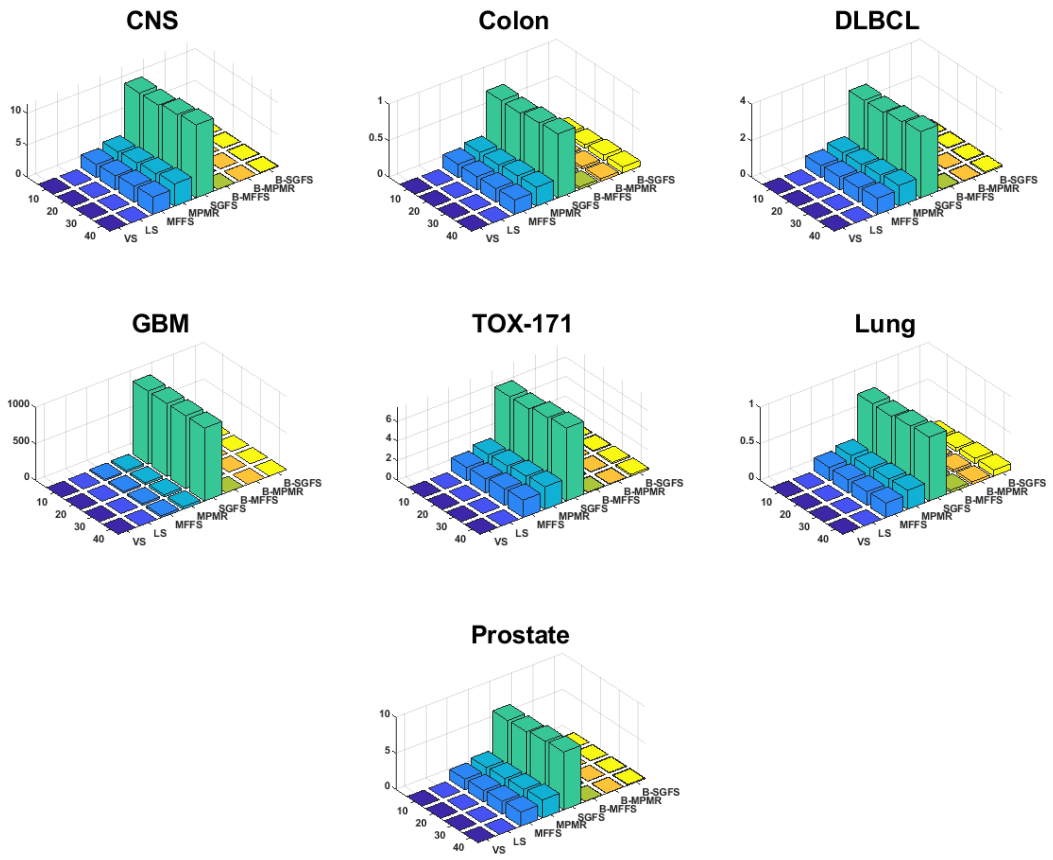

Figure 8: The CPU time of all conventional methods on seven datasets.

Figure 8 shows the running time corresponding to all the proposed algorithms is shorter compared to all the conventional methods with two exceptions including VS and LS over both Colon and TOX-171. On Colon, the running time of all the three proposed methods are slightly longer than that of VS and LS. Considering TOX-171, only the running time of B-SGFS is slightly longer than VS and LS. One reason for these exceptions is the amount of calculations compared to the level of computation corresponding to VS and LS. The most significant finding that Figure 8 provides is that all the proposed methods are faster not only than VS and LS on the rest of the datasets (Colon and TOX-171 are excepted), but also than their corresponding conventional methods, MFFS, MPMR and SGFS, over all datasets. This means that applying the notion of basis to modify MFFS, MPMR and SGFS succeeds to enhance these methods in terms of their running time. The reason for such an improvement lies in the fact that representing the original data by a basis of the feature space reduces both the redundancy among the features and the consequent level of computations. Hence, the proposed methods present modifications of the corresponding conventional methods in terms of the amount of calculations and running time as well as improving their performance as mentioned earlier.

4 Application to the Extraction of Gene Signatures for Drug Responses in Cancer

Over the last recent years, dimensionality reduction techniques and feature selection methods have been applied to a variety of real-world problems in different fields, particularly to large molecular and clinical data including gene expression datasets [58, 59]. For instance, to study complex diseases such as cancer from a molecular perspective, it is required to reduce the dimension of the molecular data and to deal with the noise and redundancy included in such types of data. In this regard, a combination of molecular signature approaches with feature selection and reduction techniques can substantially help to provide new solutions.

In this section, the newly developed methods, B-MFFS, B-MPMR and B-SGFS, are incorporated into gene signature extraction to develop an analytical framework for cancer cell lines' responses to Nilotinib treatment. In addition, the efficiency and productivity of these methods are evaluated using the CCLE dataset [55]. Furthermore, the proposed methods are compared to MFFS, MPMR and SGFS in terms of their performance.

4.1 Computational Experimental Metrics

To assess the proposed methods in terms of their classification performance and to corroborate their efficiency and efficacy, three types of evaluation metric including the classification accuracy (ACC), the true positive rate (TPR) and the true negative rate (TNR) are employed. For a given dataset, these metrics are defined as:

$$\mathrm{ACC} = \frac{\mathrm{n_{correct}}}{\mathrm{n}}, \qquad \mathrm{TPR} = \frac{\mathrm{TP}}{\mathrm{P}} \qquad \text{and} \qquad \mathrm{TNR} = \frac{\mathrm{TN}}{\mathrm{N}},$$

where n and n_{correct} indicate the numbers of the whole samples and the correct classified samples, respectively. Moreover, TP denotes the number of true positive samples, TN is the number of true negative samples, P indicates the number of positive samples and N is the number of negative samples.

The selected gene sets discovered by our proposed methods in each run have different sizes, specifically, the number of the selected genes is set to $k = 2, 5, 10$. It should be pointed out that when the feature selection process is completed, the methods used for feature selection are appraised in terms of their performance making use of the Support Vector Machine (SVM) classifier. To draw a comparison between the proposed and the benchmark feature selection techniques, a 10-fold cross-validation (CV) process is applied such that the whole dataset is randomly split into 10 groups in each CV process iteration. Then, nine of these groups are used to handle the classifier training phase and the remaining one is utilized to perform the testing phase so that the generalization ability of the trained classifier to make accurate predictions of unseen samples is guaranteed. The tuning process for setting the hyper-parameters of the methods in the training phase is guided in each iteration by an internal five-fold CV grid search on the values presented in Subsection 3.2.

4.2 Results and Discussion

The experimental results regarding the performance of the proposed techniques and its comparison with that of the benchmark methods are illustrated in Figures 9 and 10. It can be seen from Figure 9 that the bar charts of ACC and TNR corresponding to the proposed methods B-MFFS, B-MPMR and B-SGFS show a far better performance compared to that of the conventional techniques MFFS, MPMR and SGFS. It is only in the case of TPR that the performance of the proposed methods is at a

level the same as the conventional methods or is a bit lower than the performance of those techniques for some values of k. Furthermore, in terms of ACC and TPR, B-MPMR outperforms B-SGFS and B-MFFS, while in terms of TNR, B-SGFS performs better than the two other methods for $k = 2, 10$ and B-MFFS has a better performance when $k = 5$.

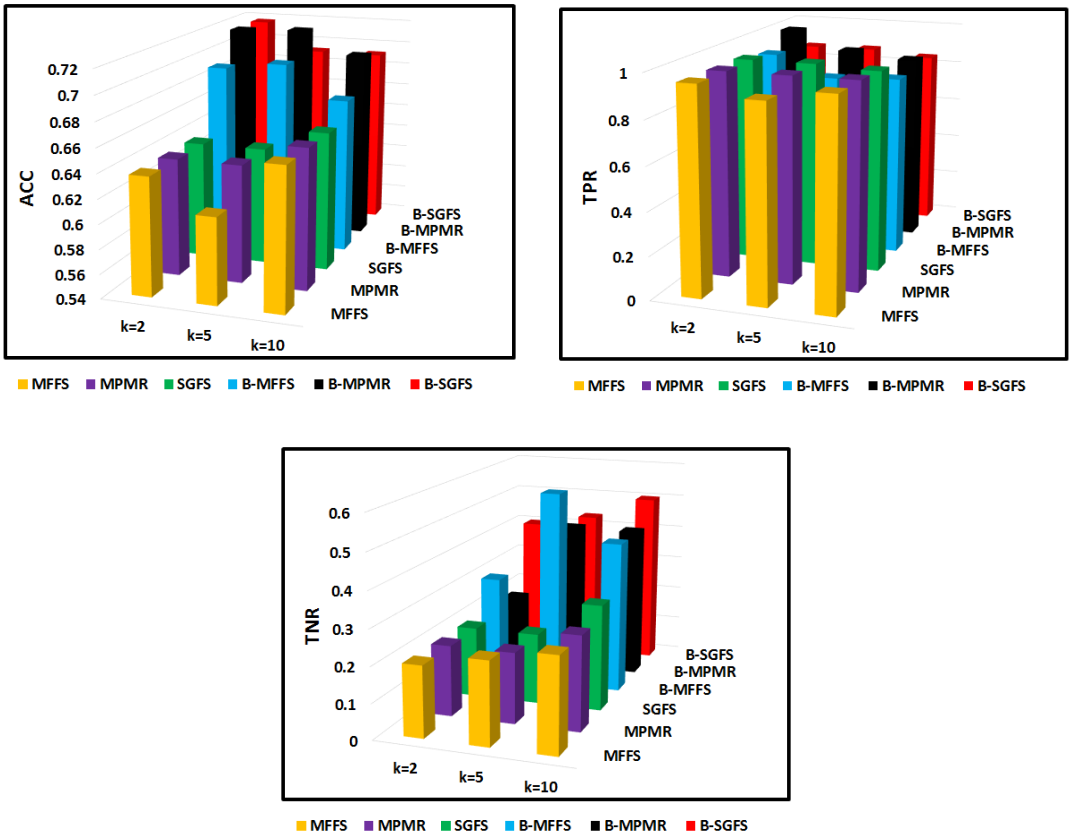

Figure 9: Bar chart of the ACC, TPR and TNR results with the number of selected features $k \in \{2, 5, 10\}$ and for different feature selection methods on the CCLE dataset. Note that a higher ACC, TPR and TNR value is indicative of a better classification performance.

Moving to Figure 10, it is clear that each of B-MFFS and B-MPMR outperforms their corresponding conventional method. It should be indicated that in the radar charts presented in Figure 10, a higher level of symmetry and a larger area of a chart are indicative of a better performance. The B-SGFS technique has also a higher performance compared to with SGFS in terms of both the ACC and TNR metrics. In addition, B-MPMR shows the best performance among all the three proposed methods.

Overall, the outcomes of experiments demonstrate that the performance of the proposed methods in terms of TNR are far better than that of the conventional methods. Moreover, the results clearly indicate that incorporation of the notion of a basis into MFFS, MPMR and SGFS is completely effective.

4.3 Verification of the Feature Selections in Therapeutic Responses to Nilotinib

Oxidative response is one of the pathways activated upon Tyrosine Kinase Inhibitors (TKI) treatment in cells [60, 61, 62]. We used the gene sets assigned to Oxidative Response in cells from Molecular

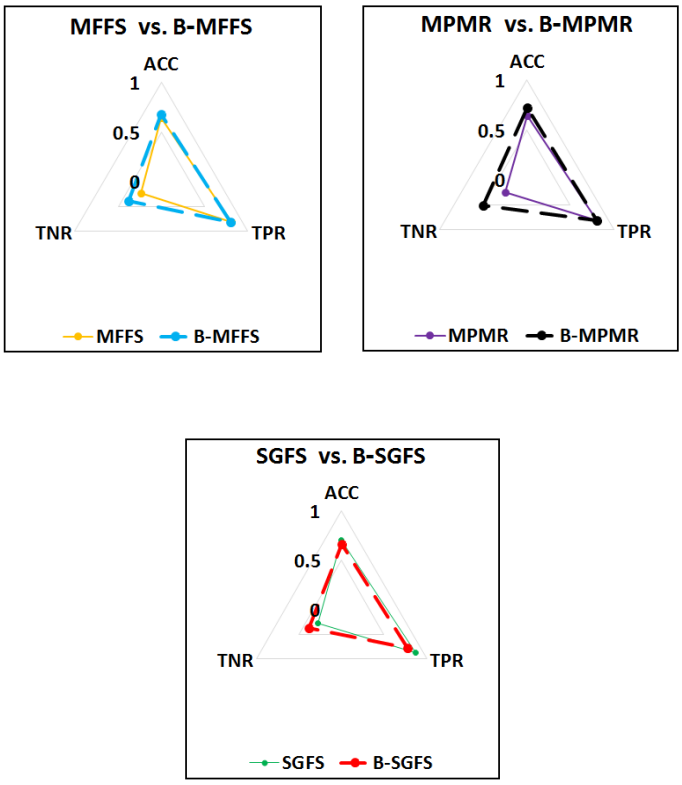

Figure 10: Results of comparison between "the MFFS and B-MFFS methods", "the MPMR and B-MPMR methods", and "the SGFS and B-SGFS methods" in respect of the metrics ACC and NMI. Each metric is represented by a vertex in the radar charts. Furthermore, the more symmetrical a chart is as well as the larger its area is, the higher performance the corresponding method will have.

Biology of The Cell (MBC) ontology [63]. To find a gene signature extracted from Oxidative Stress response pathway, we used the Cancer Cell Line Encyclopedia (CCLE) data on drug treatment [55]. The dataset we used contained IC_{50} for Nilotinib (a TKI inhibitor) treatment in 107 cancer cell lines IC_{50} ranges of 0.0029 to 7.98 μM) and their gene expression profiles. The aim was to find gene sets that can predict the cell lines' responses to Nilotinib in terms of $\mathrm{IC}_{50} < 4\mu M$. These gene sets were selected from oxidative stress pathway. The gene sets we discovered, had different sizes (gene numbers, $k = 2, 5, 10$). Our results show that applying B-MFFS and B-MPMR, we even can use a predictive 2-gene signatures. Table 4 shows which two genes are the most significant ones in each of these gene sets.

Table 4: 2-gene signatures selected by different feature selection methods.

	Method	Genes
$k = 2$	MFFS	*MSTN, GDF10*
	MPMR	*MSTN, GDF10*
	SGFS	*UGT2B4, GDF10*
	B-MFFS	*TNFRSF12A, YAP1*
	B-MPMR	*TNFRSF12A, YAP1*
	B-SGFS	*TNFRSF12A, YAP1*

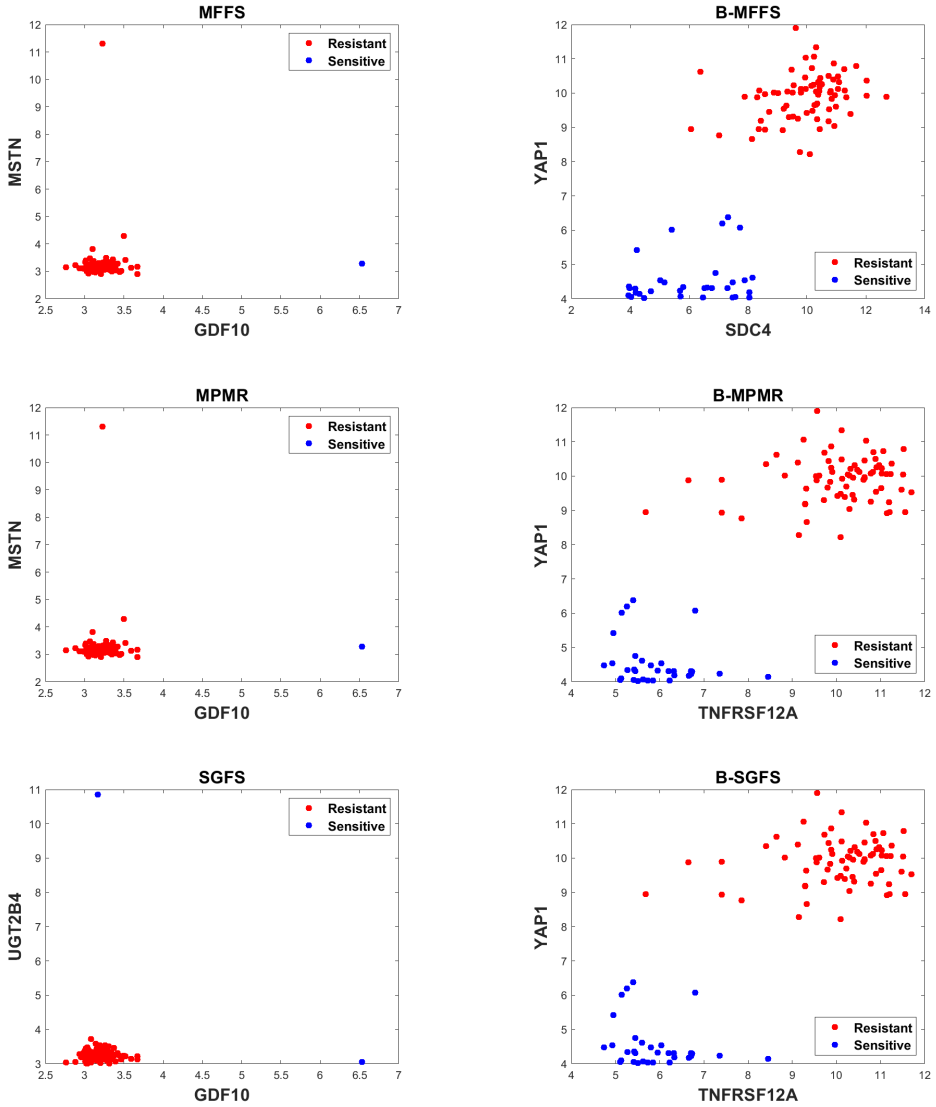

Figure 11: 2-gene signatures selected by different feature selection methods.

Figure 11 illustrates how the proposed techniques, B-MFFS, B-MPMR and B-SGFS, and their corresponding conventional methods differentiate resistant cases from sensitive ones (using $\mathrm{IC}_{50} = 4\mu M$ as a threshold) with respect to two genes selected by each one of these methods as the selected features. It is apparent from Figure 11 that while MFFS, MPMR and SGFS are not able to clearly distinguish between the two categories of resistant and sensitive cases, the proposed methods carry out this task in a highly satisfying manner. All three B-MFFS, B-MPMR and B-SGFS techniques selected *TNFRSF12A* and *YAP1* while MFFS and MPMR selected *MSTN* and *GDF10* as the selected 2-gene signature. SGFS found *GDF10* and *UGT2B4* as selected features for a 2-gene signature. It has been shown that both *TNFRSF12A* and *YAP1* are involved in TKI treatment responsiveness in cancer [64, 65, 66, 67].

5 Conclusion

High-dimensional data analysis is a foundation for systems approaches in medicine [68]. The applicability of these approaches in the real-world settings requires high dimensionality reduction [68]. This reduction helps to build predictive models in systems pharmacology of cancer to optimize therapeutic regimens proposed by *in vivo* and *in vitro* experiments [69]. Our results showed that our modified version of feature selection methods based on matrix factorization, we call B-MFFS, B-MPMR, and B-SGFS, could reduce the dimensionality of different datasets and provide feature signatures with higher accuracy than conventional methods. This is very important in the practice of quantitative and systems pharmacology, where we need to build both mechanistic and phenomenological models that emerge from omic data [70, 71]. To translate big complex data of omics and multi-omics into applied models for *in vitro*, *in vivo*, and clinical validation, we need such methodologies. This high dimensionality reduction can pave the path to establishing integrated systems pharmacology platforms that can predict drug responses in cancer cell lines and tumor models using small sets of bio-molecular markers [70].

One of the most potent applications of systems pharmacology is using dynamical models of signaling networks. These signaling networks consist of complex interactions among a large number of proteins or genes [72]. One of the primary practices to build and tune these models is to use prior biological knowledge to construct a reduced version of these interactions [72]. Our proposed methods can reduce these feature spaces quantitatively and select the most significant nodes in the interaction networks for more accurate and realistic dynamical models. The huge parameter spaces of these models also need reduction to represent a robust, optimized model [9]. Our dimensionality reduction methods can be applied to solve this problem as well.

Besides dynamic models, finding molecular sets to predict therapeutic responses in cancer models is an unmet need, and quantitative modalities like our proposed methodologies can provide the principles for this complex challenge.

Author Contributions

A.M., I.T., F.S.M. and M.E., conceived the project. A.M., F.S.M., N.A., M.R.R., I.T., and M.E. designed the computational methodology. A.M., F.S.M., M.R.R., and I.T. did the computational analysis. All authors read and commented on the manuscript.

Acknowledgments

This research is financially supported by Iran National Science Foundation (INSF) and Shahid Bahonar University of Kerman [grant number: 97021946]. I.T. contributed to this paper at the Cellular Energetics Program of the Kavli Institute for Theoretical Physics, supported in part by the National Science Foundation Grant NSF PHY-1748958, NIH Grant R25GM067110, and the Gordon and Betty Moore Foundation Grant 2919.02.

Abbreviations

ACC, Clustering Accuracy; CCLE, Cancer Cell Line Encyclopedia; DLBCL, Diffuse large B-cell lymphoma; GB, Glioblastoma Multiforme; LS, Laplacian Score; MBC, Molecular Biology of The Cell;

MFFS, matrix factorization; MPMR, Maximum Projection and Minimum Redundancy; NMF, Non-negative Matrix Factorization; NMI, Normalized Mutual Information; PCA, Principal Components Analysis; SGFS, Subspace learning-based Graph Regularized Feature Selection; SVD, Singular Value Decomposition; TKI, Tyrosine Kinase Inhibitor; TPR, True Positive Rate; TNR, True Negative Rate; VS, Variance Score.

References

[1] Iman Tavassoly, Joseph Goldfarb, and Ravi Iyengar. Systems biology primer: the basic methods and approaches. *Essays in biochemistry*, 62(4):487–500, 2018.

[2] Iman Tavassoly, Yuan Hu, Shan Zhao, Chiara Mariottini, Aislyn Boran, Yibang Chen, Lisa Li, Rosa E Tolentino, Gomathi Jayaraman, Joseph Goldfarb, et al. Genomic signatures defining responsiveness to allopurinol and combination therapy for lung cancer identified by systems therapeutics analyses. *Molecular oncology*, 13(8):1725–1743, 2019.

[3] Prashant Dogra, Joseph D Butner, Yao-li Chuang, Sergio Caserta, Shreya Goel, C Jeffrey Brinker, Vittorio Cristini, and Zhihui Wang. Mathematical modeling in cancer nanomedicine: a review. *Biomedical Microdevices*, 21(2):1–23, 2019.

[4] Shigeyuki Magi, Kazunari Iwamoto, and Mariko Okada-Hatakeyama. Current status of mathematical modeling of cancer–from the viewpoint of cancer hallmarks. *Current Opinion in Systems Biology*, 2:39–48, 2017.

[5] Miguel Ángel Medina. Mathematical modeling of cancer metabolism. *Critical reviews in oncology/hematology*, 124:37–40, 2018.

[6] Tayebeh Waezizadeh, Adel Mehrpooya, Maryam Rezaeizadeh, and Shantia Yarahmadian. Mathematical models for the effects of hypertension and stress on kidney and their uncertainty. *Mathematical biosciences*, 305:77–95, 2018.

[7] Iman Tavassoly. *Dynamics of Cell Fate Decision Mediated by the Interplay of Autophagy and Apoptosis in Cancer Cells: Mathematical Modeling and Experimental Observations*. Springer, 2015.

[8] Mohammadreza Dorvash, Mohammad Farahmandnia, and Iman Tavassoly. A systems biology roadmap to decode mtor control system in cancer. *Interdisciplinary Sciences: Computational Life Sciences*, 12(1):1–11, 2020.

[9] I Tavassoly, J Parmar, AN Shajahan-Haq, R Clarke, William T Baumann, and John J Tyson. Dynamic modeling of the interaction between autophagy and apoptosis in mammalian cells. *CPT: pharmacometrics & systems pharmacology*, 4(4):263–272, 2015.

[10] Evanthia Koukouli, Dennis Wang, Frank Dondelinger, and Juhyun Park. A regularized functional regression model enabling transcriptome-wide dosage-dependent association study of cancer drug response. *PLoS computational biology*, 17(1):e1008066, 2021.

[11] Mehrdad Rostami, Kamal Berahmand, Elahe Nasiri, and Saman Forouzande. Review of swarm intelligence-based feature selection methods. *Engineering Applications of Artificial Intelligence*, 100:104210, 2021.

[12] Dong Wang, Jin-Xing Liu, Ying-Lian Gao, Chun-Hou Zheng, and Yong Xu. Characteristic gene selection based on robust graph regularized non-negative matrix factorization. *IEEE/ACM transactions on computational biology and bioinformatics*, 13(6):1059–1067, 2015.

[13] Jean-Philippe Brunet, Pablo Tamayo, Todd R Golub, and Jill P Mesirov. Metagenes and molecular pattern discovery using matrix factorization. *Proceedings of the national academy of sciences*, 101(12):4164–4169, 2004.

[14] Karthik Devarajan. Nonnegative matrix factorization: an analytical and interpretive tool in computational biology. *PLoS Comput Biol*, 4(7):e1000029, 2008.

[15] Raffaele Giancarlo and Filippo Utro. Speeding up the consensus clustering methodology for microarray data analysis. *Algorithms for Molecular Biology*, 6(1):1–13, 2011.

[16] Belhassen Bayar, Nidhal Bouaynaya, and Roman Shterenberg. Probabilistic non-negative matrix factorization: theory and application to microarray data analysis. *Journal of bioinformatics and computational biology*, 12(01):1450001, 2014.

[17] Isabelle Guyon, Jason Weston, Stephen Barnhill, and Vladimir Vapnik. Gene selection for cancer classification using support vector machines. *Machine learning*, 46(1):389–422, 2002.

[18] Yue Li and Zhaolei Zhang. Computational biology in microrna. *Wiley Interdisciplinary Reviews: RNA*, 6(4):435–452, 2015.

[19] Jin-Xing Liu, Yong Xu, Chun-Hou Zheng, Heng Kong, and Zhi-Hui Lai. Rpca-based tumor classification using gene expression data. *IEEE/ACM Transactions on Computational Biology and Bioinformatics*, 12(4):964–970, 2014.

[20] Haifa Ben Saber and Mourad Elloumi. Dna microarray data analysis: a new survey on biclustering. *International Journal for Computational Biology (IJCB)*, 4(1):21–37, 2015.

[21] Chun-Hou Zheng, Lei Zhang, To-Yee Ng, Chi Keung Shiu, and De-Shuang Huang. Metasample-based sparse representation for tumor classification. *IEEE/ACM Transactions on Computational Biology and Bioinformatics*, 8(5):1273–1282, 2011.

[22] Verónica Bolón-Canedo, Noelia Sánchez-Maroño, and Amparo Alonso-Betanzos. A review of feature selection methods on synthetic data. *Knowledge and information systems*, 34(3):483–519, 2013.

[23] Isabelle Guyon, Steve Gunn, Masoud Nikravesh, and Lofti A Zadeh. *Feature extraction: foundations and applications*, volume 207. Springer, 2008.

[24] Zena M Hira and Duncan F Gillies. A review of feature selection and feature extraction methods applied on microarray data. *Advances in bioinformatics*, 2015, 2015.

[25] Alexandros Kalousis, Julien Prados, and Melanie Hilario. Stability of feature selection algorithms: a study on high-dimensional spaces. *Knowledge and information systems*, 12(1):95–116, 2007.

[26] Mehrdad Rostami, Saman Forouzandeh, Kamal Berahmand, and Mina Soltani. Integration of multi-objective pso based feature selection and node centrality for medical datasets. *Genomics*, 112(6):4370–4384, 2020.

[27] Jun Chin Ang, Andri Mirzal, Habibollah Haron, and Haza Nuzly Abdull Hamed. Supervised, unsupervised, and semi-supervised feature selection: a review on gene selection. *IEEE/ACM transactions on computational biology and bioinformatics*, 13(5):971–989, 2015.

[28] Verónica Bolón-Canedo, Noelia Sánchez-Marono, Amparo Alonso-Betanzos, José Manuel Benítez, and Francisco Herrera. A review of microarray datasets and applied feature selection methods. *Information Sciences*, 282:111–135, 2014.

[29] Mahla Mokhtia, Mahdi Eftekhari, and Farid Saberi-Movahed. Feature selection based on regularization of sparsity based regression models by hesitant fuzzy correlation. *Applied Soft Computing*, 91:106255, 2020.

[30] Jie Cai, Jiawei Luo, Shulin Wang, and Sheng Yang. Feature selection in machine learning: A new perspective. *Neurocomputing*, 300:70–79, 2018.

[31] Mahdi Eftekhari, Farid Saberi-Movahed, and Adel Mehrpooya. Supervised feature selection via information gain, maximum projection and minimum redundancy. In *SLAA10 Seminar Linear Algebra and Its Application*, pages 29–35, 2020.

[32] Ronghua Shang, Jiuzheng Song, Licheng Jiao, and Yangyang Li. Double feature selection algorithm based on low-rank sparse non-negative matrix factorization. *International Journal of Machine Learning and Cybernetics*, pages 1–18, 2020.

[33] Jianglin Lu, Hailing Wang, Jie Zhou, Yudong Chen, Zhihui Lai, and Qinghua Hu. Low-rank adaptive graph embedding for unsupervised feature extraction. *Pattern Recognition*, 113:107758, 2021.

[34] Miao Qi, Ting Wang, Fucong Liu, Baoxue Zhang, Jianzhong Wang, and Yugen Yi. Unsupervised feature selection by regularized matrix factorization. *Neurocomputing*, 273:593–610, 2018.

[35] Farid Saberi-Movahed, Mahdi Eftekhari, and Mohammad Mohtashami. Supervised feature selection by constituting a basis for the original space of features and matrix factorization. *International Journal of Machine Learning and Cybernetics*, 11:1405–1421, 2020.

[36] Ronghua Shang, Kaiming Xu, Fanhua Shang, and Licheng Jiao. Sparse and low-redundant subspace learning-based dual-graph regularized robust feature selection. *Knowledge-Based Systems*, 187:104830, 2020.

[37] Shiping Wang, Witold Pedrycz, Qingxin Zhu, and William Zhu. Subspace learning for unsupervised feature selection via matrix factorization. *Pattern Recognition*, 48(1):10–19, 2015.

[38] Shiping Wang, Witold Pedrycz, Qingxin Zhu, and William Zhu. Unsupervised feature selection via maximum projection and minimum redundancy. *Knowledge-Based Systems*, 75:19–29, 2015.

[39] Ronghua Shang, Wenbing Wang, Rustam Stolkin, and Licheng Jiao. Subspace learning-based graph regularized feature selection. *Knowledge-Based Systems*, 112:152–165, 2016.

[40] Gene H Golub and Christian Reinsch. Singular value decomposition and least squares solutions. In *Linear algebra*, pages 134–151. Springer, 1971.

[41] Daniel D Lee and H Sebastian Seung. Learning the parts of objects by non-negative matrix factorization. *Nature*, 401(6755):788–791, 1999.

[42] I.T. Jolliffe. *Principal Component Analysis*. Springer, 1986.

[43] Feiping Nie, Heng Huang, Xiao Cai, and Chris Ding. Efficient and robust feature selection via joint $l_{2,1}$-norm minimization. *Advances in neural information processing systems*, 23:1813–1821, 2010.

[44] Khadidja Henni, Neila Mezghani, and Charles Gouin-Vallerand. Unsupervised graph-based feature selection via subspace and pagerank centrality. *Expert Systems with Applications*, 114:46–53, 2018.

[45] Shaoyong Li, Chang Tang, Xinwang Liu, Yaping Liu, and Jiajia Chen. Dual graph regularized compact feature representation for unsupervised feature selection. *Neurocomputing*, 331:77–96, 2019.

[46] Chang Tang, Meiru Bian, Xinwang Liu, Miaomiao Li, Hua Zhou, Pichao Wang, and Hailin Yin. Unsupervised feature selection via latent representation learning and manifold regularization. *Neural Networks*, 117:163–178, 2019.

[47] André Gaul. *Recycling Krylov subspace methods for sequences of linear systems: Analysis and applications*. PhD thesis, Technischen Universit at Berlin, 2014.

[48] A El Guennouni, Khalide Jbilou, and AJ Riquet. Block Krylov subspace methods for solving large Sylvester equations. *Numerical Algorithms*, 29(1-3):75–96, 2002.

[49] Mohammed Heyouni and Azeddine Essai. Matrix Krylov subspace methods for linear systems with multiple right-hand sides. *Numerical Algorithms*, 40(2):137–156, 2005.

[50] Scott L Pomeroy, Pablo Tamayo, Michelle Gaasenbeek, Lisa M Sturla, Michael Angelo, Margaret E McLaughlin, John YH Kim, Liliana C Goumnerova, Peter M Black, Ching Lau, et al. Prediction of central nervous system embryonal tumour outcome based on gene expression. *Nature*, 415(6870):436–442, 2002.

[51] Uri Alon, Naama Barkai, Daniel A Notterman, Kurt Gish, Suzanne Ybarra, Daniel Mack, and Arnold J Levine. Broad patterns of gene expression revealed by clustering analysis of tumor and normal colon tissues probed by oligonucleotide arrays. *Proceedings of the National Academy of Sciences*, 96(12):6745–6750, 1999.

[52] Ash A Alizadeh, Michael B Eisen, R Eric Davis, Chi Ma, Izidore S Lossos, Andreas Rosenwald, Jennifer C Boldrick, Hajeer Sabet, Truc Tran, Xin Yu, et al. Distinct types of diffuse large b-cell lymphoma identified by gene expression profiling. *Nature*, 403(6769):503–511, 2000.

[53] William A Freije, F Edmundo Castro-Vargas, Zixing Fang, Steve Horvath, Timothy Cloughesy, Linda M Liau, Paul S Mischel, and Stanley F Nelson. Gene expression profiling of gliomas strongly predicts survival. *Cancer research*, 64(18):6503–6510, 2004.

[54] Jundong Li, Kewei Cheng, Suhang Wang, Fred Morstatter, Robert P Trevino, Jiliang Tang, and Huan Liu. Feature selection: A data perspective. *ACM Computing Surveys (CSUR)*, 50(6):94, 2018.

[55] Jordi Barretina, Giordano Caponigro, Nicolas Stransky, Kavitha Venkatesan, Adam A Margolin, Sungjoon Kim, Christopher J Wilson, Joseph Lehár, Gregory V Kryukov, Dmitriy Sonkin, et al. The cancer cell line encyclopedia enables predictive modelling of anticancer drug sensitivity. *Nature*, 483(7391):603–607, 2012.

[56] Christopher M Bishop et al. *Neural networks for pattern recognition*. Oxford university press, 1995.

[57] Xiaofei He, Deng Cai, and Partha Niyogi. Laplacian score for feature selection. *Advances in neural information processing systems*, 18:507–514, 2005.

[58] Verónica Bolón-Canedo, Noelia Sánchez-Maroño, and Amparo Alonso-Betanzos. On the effectiveness of discretization on gene selection of microarray data. In *The 2010 International Joint Conference on Neural Networks (IJCNN)*, pages 1–8. IEEE, 2010.

[59] Yvan Saeys, Inaki Inza, and Pedro Larranaga. A review of feature selection techniques in bioinformatics. *bioinformatics*, 23(19):2507–2517, 2007.

[60] Katherine M Aird, Jennifer L Allensworth, Ines Batinic-Haberle, H Kim Lyerly, Mark W Dewhirst, and Gayathri R Devi. Erbb1/2 tyrosine kinase inhibitor mediates oxidative stress-induced apoptosis in inflammatory breast cancer cells. *Breast cancer research and treatment*, 132(1):109–119, 2012.

[61] Marija Mihajlovic, Branka Ivkovic, Biljana Jancic-Stojanovic, Aleksandra Zeljkovic, Vesna Spasojevic-Kalimanovska, Jelena Kotur-Stevuljevic, and Dragana Vujanovic. Modulation of oxidative stress/antioxidative defence in human serum treated by four different tyrosine kinase inhibitors. *Anti-cancer drugs*, 31(9):942–949, 2020.

[62] Mohamed E Shaker. Nilotinib interferes with the signalling pathways implicated in acetaminophen hepatotoxicity. *Basic & clinical pharmacology & toxicology*, 114(3):263–270, 2014.

[63] Jens Hansen, David Meretzky, Simeneh Woldesenbet, Gustavo Stolovitzky, and Ravi Iyengar. A flexible ontology for inference of emergent whole cell function from relationships between subcellular processes. *Scientific reports*, 7(1):1–13, 2017.

[64] Jesper B Andersen, Bart Spee, Boris R Blechacz, Itzhak Avital, Mina Komuta, Andrew Barbour, Elizabeth A Conner, Matthew C Gillen, Tania Roskams, Lewis R Roberts, et al. Genomic and genetic characterization of cholangiocarcinoma identifies therapeutic targets for tyrosine kinase inhibitors. *Gastroenterology*, 142(4):1021–1031, 2012.

[65] Soon Auck Hong, Si-Hyong Jang, Mee-Hye Oh, Sung Joon Kim, Jin-Hyung Kang, and Sook-Hee Hong. Overexpression of yap1 in egfr mutant lung adenocarcinoma prior to tyrosine kinase inhibitor therapy is associated with poor survival. *Pathology-Research and Practice*, 214(3):335–342, 2018.

[66] Jai-Nien Tung, Po-Lin Lin, Yao-Chen Wang, De-Wei Wu, Chi-Yi Chen, and Huei Lee. Pd-l1 confers resistance to egfr mutation-independent tyrosine kinase inhibitors in non-small cell lung cancer via upregulation of yap1 expression. *Oncotarget*, 9(4):4637, 2018.

[67] Timothy G Whitsett, Emily Cheng, Landon Inge, Kaushal Asrani, Nathan M Jameson, Galen Hostetter, Glen J Weiss, Christopher B Kingsley, Joseph C Loftus, Ross Bremner, et al. Elevated expression of fn14 in non-small cell lung cancer correlates with activated egfr and promotes tumor cell migration and invasion. *The American journal of pathology*, 181(1):111–120, 2012.

[68] Charles Auffray, Zhu Chen, and Leroy Hood. Systems medicine: the future of medical genomics and healthcare. *Genome medicine*, 1(1):1–11, 2009.

[69] Iman Tavassoly, Yuan Hu, Shan Zhao, Chiara Mariottini, Aislyn Boran, Yibang Chen, Lisa Li, Rosa E Tolentino, Gomathi Jayaraman, Joseph Goldfarb, et al. Genomic signatures defining responsiveness to allopurinol and combination therapy for lung cancer identified by systems therapeutics analyses. *Molecular oncology*, 13(8):1725–1743, 2019.

[70] Iman Tavassoly, Joseph Goldfarb, and Ravi Iyengar. Systems biology primer: the basic methods and approaches. *Essays in biochemistry*, 62(4):487–500, 2018.

[71] Piet H Van der Graaf and Neil Benson. Systems pharmacology: bridging systems biology and pharmacokinetics-pharmacodynamics (pkpd) in drug discovery and development. *Pharmaceutical research*, 28(7):1460–1464, 2011.

[72] John J Tyson, William T Baumann, Chun Chen, Anael Verdugo, Iman Tavassoly, Yue Wang, Louis M Weiner, and Robert Clarke. Dynamic modelling of oestrogen signalling and cell fate in breast cancer cells. *Nature Reviews Cancer*, 11(7):523–532, 2011.

[73] Valeria Simoncini. Computational methods for linear matrix equations. *SIAM Review*, 58(3):377–441, 2016.

[74] Carl D Meyer. *Matrix analysis and applied linear algebra*, volume 71. SIAM, 2000.

Appendix

A Global conjugate gradient method

The global conjugate gradient method was developed as an extension of the conjugate gradient technique [49, 73]. Over the past recent years, it has been demonstrated that comparing to direct techniques

such as the Gaussian elimination method, the iterative technique of global conjugate gradient enjoys a far better performance to deal with large matrix equations. In such cases, it is usually supposed that constraints such as being both sparse and symmetric positive definite are imposed on the coefficient matrix corresponding to the given matrix equation [47]. A basic form of matrix equations whose exact solution can be estimated by this method is

$$\mathbf{A}_1\mathbf{X}\mathbf{B}_1 + \mathbf{A}_2\mathbf{X}\mathbf{B}_2 + \cdots + \mathbf{A}_p\mathbf{X}\mathbf{B}_p = \mathbf{C}, \tag{25}$$

in which the matrices $\mathbf{A}_j \in \mathbb{R}^{n\times n}$ and $\mathbf{B}_j \in \mathbb{R}^{m\times m}$ are symmetric positive definite (or symmetric semi-positive definite) for $j = 1, \ldots, p$ and $\mathbf{C} \in \mathbb{R}^{n\times m}$. The unknown matrix is denoted by $\mathbf{X} \in \mathbb{R}^{n\times m}$. Algorithm A1 presents the global conjugate gradient framework.

Algorithm A1 The global conjugate gradient method.

Input: The matrices $\mathbf{A}_j \in \mathbb{R}^{n\times n}$, $\mathbf{B}_j \in \mathbb{R}^{m\times m}$, for $j = 1, \ldots, p$, the right-hand side $\mathbf{C} \in \mathbb{R}^{n\times m}$, an initial guess $\mathbf{X}_0 \in \mathrm{R}^{n\times m}$, a tolerance ϵ and the maximum number of iterations *maxIter*.

Output: Return $\mathbf{X}_k$ as the approximate solution of (25).

1: Set $\mathcal{M}(\mathbf{X}) = \mathbf{A}_1\mathbf{X}\mathbf{B}_1 + \mathbf{A}_2\mathbf{X}\mathbf{B}_2 + \cdots + \mathbf{A}_p\mathbf{X}\mathbf{B}_p$.
2: Set $\mathbf{R}_0 = \mathbf{C} - \mathcal{M}(\mathbf{X}_0)$, and $\mathbf{P}_0 = \mathbf{R}_0$.
3: **for** $k = 1, \ldots,$ *maxIter* **do**
4: Compute $\alpha_{k-1} = \frac{\|\mathbf{R}_{k-1}\|_F^2}{\mathrm{Tr}(\mathbf{P}_{k-1}^T\mathcal{M}(\mathbf{P}_{k-1}))}$.
5: Compute $\mathbf{X}_k = \mathbf{X}_{k-1} + \alpha_{k-1}\mathbf{P}_{k-1}$, and $\mathbf{R}_k = \mathbf{R}_{k-1} - \alpha_{k-1}\mathcal{M}(\mathbf{P}_{k-1})$.
6: If $\|\mathbf{R}_{k+1} - \mathbf{R}_k\|_F < \epsilon$ then return $\mathbf{X}_k$.
7: Compute $\beta_k = \frac{\|\mathbf{R}_k\|_F^2}{\|\mathbf{R}_{k-1}\|_F^2}$, and $\mathbf{P}_k = \mathbf{R}_k + \beta_k\mathbf{P}_{k-1}$.
8: **end for**

B Basis extension technique

In linear algebra, the extension method is a standard commonly used technique to produce a basis of a given vector space when the dimension of the space is finite [74]. For an $n\times d$ matrix $\mathbf{V} = [\mathbf{v}_1, \ldots, \mathbf{v}_d]$, where $1 < \mathrm{rank}(\mathbf{V}) = p \leq \min\{n, d\}$, it is assumed that $V_1 = \{\mathbf{v}_{i_1}\}$ and which $\mathbf{v}_{i_1} \in \{\mathbf{v}_1, \ldots, \mathbf{v}_d\}$ is not the zero vector of size n. Therefore, the subset V_1 is linearly independent. Now considering $1 < p$, a vector $\mathbf{v}_{i_2} \in \{\mathbf{v}_1, \ldots, \mathbf{x}_d\} - \mathrm{span}(V_1)$ can be found. It is evident that the extension of V_1 defined as $V_2 = V_1 \cup \{\mathbf{v}_{i_2}\} = \{\mathbf{v}_{i_1}, \mathbf{v}_{i_2}\}$ is a linearly independent subset. Now, continuing this process, a series $V_3, V_4, \ldots, V_p$ of subsets that are linearly independent extensions of V_1 is obtained. Considering the fact that V_p is composed of p vectors, V_p is a basis of $\mathcal{V} = \mathrm{span}\{\mathbf{v}_1, \ldots, \mathbf{v}_d\}$. Algorithm B1 summarizes the extension technique procedure to construct a basis for $\mathrm{span}(\mathbf{V})$.

Algorithm B1 The basis extension technique [74].

Input: Data matrix $\mathbf{V} = [\mathbf{v}_1, \mathbf{v}_2, \ldots, \mathbf{v}_d] \in \mathbb{R}^{n \times d}$ such that $1 < \mathrm{rank}(\mathbf{V}) = p \leq \min\{n, d\}$.
Output: A basis B for $\mathcal{V} = \mathrm{span}(\mathbf{V})$.

```
Choose an element of {v_1, ..., v_d} such as {v_{i_1}}. Set B = {v_{i_1}}.
for k = 2 : n do
    Find a vector v_{i_k} ∈ V in a way that v_{i_k} ∉ span(B). Set B ← B ∪ {v_{i_k}}.
end for
```